12

Diamond Spectroscopy, Defect Centers, Color, and Treatments

Ben L. Green

Department of Physics
University of Warwick
Coventry CV4 7AL, UK

Alan T. Collins

Department of Physics
King's College London
Strand
London WC2R 2LS, UK

Christopher M. Breeding

Gemological Institute of America
The Robert Mouawad Campus
5345 Armada Drive
Carlsbad, CA92008, USA

b.green@warwick.ac.uk; alan.collins@kcl.ac.uk; mbreedin@gia.edu

OPTICAL SPECTROSCOPY OF DEFECT-FREE DIAMOND

Optical spectroscopy is a valuable non-destructive technique for the study of many materials. For diamond it is used for fundamental research to enhance our knowledge about this remarkable material; it is used in gem-testing laboratories to determine whether a diamond is natural or synthetic and whether its color is natural or has been enhanced by treatment; and it is used in the characterization and selection of diamonds for certain high-technology applications—laser windows, for example.

The nature of light

The study of a material's spectral interaction with light is known as optical spectroscopy, and we can begin by asking the simple question, "What is light?". The light that we observe with our eyes (and also the light that we can't see) is due to the propagation of energy in space as a combination of electric and magnetic fields, known as an *electromagnetic wave*. This wave can be characterized by its wavelength, and for light in the visible region the wavelengths span from 400 nm in the violet region to 700 nm in the red region. We are all familiar with the sight of a rainbow, and if the colors of the rainbow are shown on a diagram where the wavelengths increase vertically downwards, then below the red is the infrared, and above the violet we have the ultraviolet. These regions cannot be detected by the human eye, but they can be investigated using suitable instruments which are sensitive to these wavelengths. For diamond, we will find that measurements in all three regions are needed.

Light can also be regarded as a stream of *photons*. For light that has a single wavelength (and therefore a single color, i.e., *monochromatic* light), each photon has a *quantum* of energy (measured in Joules) given by

$$E = h\nu = \frac{hc}{\lambda}$$

where h is Planck's constant, ν is the frequency, c is the speed of light and λ is the wavelength. The Joule is not a very convenient unit, and in spectroscopy E is usually expressed in electron volts (eV) as

$$E = \frac{hc}{e\lambda} = \frac{1239.84}{\lambda(nm)}$$

where e is the electronic charge.

For high-precision measurements it is important to realize that the wavelength in this formula is the wavelength in a vacuum. Most measurements are made in air, and the refractive index of air must be taken into account. A more appropriate numerical factor is then

$$E \approx \frac{1239.50}{\lambda(nm)}$$

and therefore, an infrared electromagnetic wave of energy $1\,eV$ has a wavelength of 1239.50 nm in air. The approximate sign is because the refractive index of air changes slightly with temperature, pressure and wavelength.

In the infrared spectral region, and in Raman spectroscopy, the preferred unit is wavenumbers. The wavenumber $\bar{\nu}$ is given by the reciprocal of the vacuum wavelength in cm and is therefore expressed in cm^{-1}. This is equivalent to

$$\bar{\nu} = \frac{10^7}{\lambda(nm)} cm^{-1}$$

The following spectral positions (measured *in vacuo*) are therefore identical: 500.00 nm, 2.4797 eV, 20,000 cm^{-1}. We explicitly note that wavenumbers are proportional to energy, whereas wavelength is proportional to its inverse.

Phonons and Raman scattering

To interpret some of the optical spectra of diamond we need to consider the vibrations of the carbon bonds. Consider a one-dimensional crystal with the ends fixed; Figure 1 shows such a "crystal" with seven atoms. The possible frequencies of vibration are represented by one half-wavelength, two half-wavelengths, three half-wavelengths etc., up to the point where adjacent atoms are vibrating in antiphase. The last corresponds to the maximum possible frequency of vibration. The same considerations apply in a three-dimensional crystal, although the full details are more complicated than suggested by this simple model.

By analogy with light waves, we can represent a vibrational wave by a particle called a *phonon*. It is possible for photons and electrons to interact with the vibrational waves in a crystal, giving *photon–phonon* and *electron–phonon* scattering. The energy of a phonon is usually written as $\hbar\Omega$, where $\hbar$ is $h/2\pi$ and $\Omega = 2\pi\nu$ (c.f. $E = h\nu$ for a photon).

Raman scattering is an important example of the photon–phonon interaction. Incident photons with energy $h\nu$ are weakly scattered by the phonons in a crystal to produce Raman-scattered photons at energies:

$h\nu_S = h\nu - \hbar\Omega$ (phonon creation; Stokes scattering), and
$h\nu_{AS} = h\nu + \hbar\Omega$ (phonon destruction; anti-Stokes scattering).

In the first process the incoming photon loses energy and generates a vibrational wave in the crystal; in the second case the photon gains energy from vibrational waves that are already present in the material. At room temperature, and below, the anti-Stokes scattering in diamond is very weak compared with the Stokes scattering. The Raman energy of diamond

is 1332.5 cm^{-1}, and this corresponds to the maximum vibrational frequency of the diamond lattice at room temperature and lower. A Raman spectrum may be produced by using an intense monochromatic excitation source (typically a laser) and plotting the number of scattered photons versus the photon energy separation (in wavenumbers) from the photon energy of the source. Figure 2 shows the first-order Raman line at 1332 cm^{-1} and the weak, characteristic, second-order spectrum (which is not simply a single peak) with a sharp spike at 2667 cm^{-1}. As Raman scattering is intimately connected with vibrations within the crystal, a Raman microscope can be used to study compressive and tensile strain inside a crystal via shifts in the local Raman frequency (Crisci et al. 2011), and even give information on the environment surrounding a non-diamond inclusion (Howell et al. 2012).
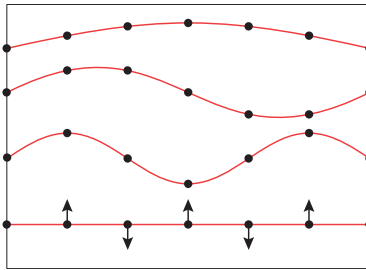
Figure 1. Illustration of the possible vibrational modes of a finite one-dimensional chain of atoms whose ends are fixed. The energy of the vibrations increases from a single half-wavelength (**top**) to nearest-neighbor atoms vibrating in antiphase (**bottom**). In a real crystal, the number of atoms, and hence vibrational modes, is of the order of 10^{14} per cubic millimeter, but we may still gain a basic but intuitive picture of crystal vibrations from this model.
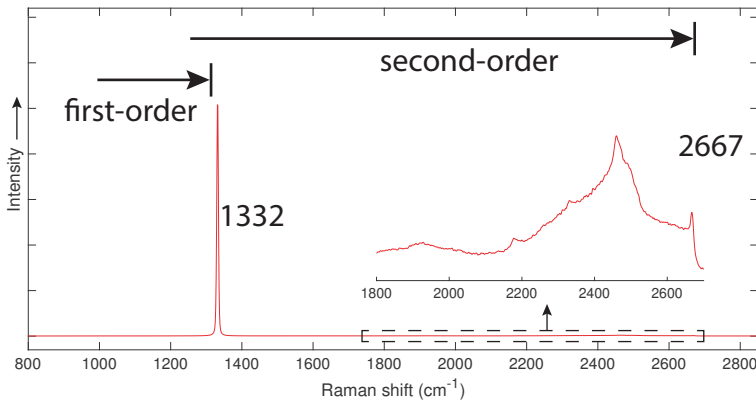
Figure 2. First- and second-order Raman spectra collected from a high-purity diamond using excitation at 514.5 nm. These spectral shapes are intrinsic to high-quality, high-purity diamond and can be used to distinguish diamond from analogues. In high-resolution spectroscopy, the width and absolute position of the Raman line can be used to analyze strain within a sample.

Optical absorption

When light is incident on one side of a transparent material, some light is reflected, and some is transmitted. If the intensities of the incident light $I_0(\lambda)$ and the transmitted light $I_t(\lambda)$ at each wavelength λ are measured, a quantity called the *absorption coefficient, α*, may be calculated at each wavelength using the expression

$$\alpha = \frac{1}{t}\log_e\left(\frac{I_0(\lambda)}{I_t(\lambda)}\right)$$

This is an approximate expression which ignores reflection at the crystal surfaces; the major effect of the approximation is to offset the zero of the absorption coefficient. The sample thickness, t, is usually measured in cm, and so the units of α are cm^{-1}.

Commercial spectrophotometers and Fourier Transform Infrared (FTIR) spectrometers usually display the output as *absorbance, A*. This is defined by

$$A = \log_{10}\left(\frac{I_0(\lambda)}{I_t(\lambda)}\right)$$

Absorbance may be converted to absorption coefficient using $\alpha = \log_e(10)A/t$. The importance of using absorption coefficient it is that is proportional to the concentration of the absorbing species and is not impacted by the thickness of the material or pathlength.

Absorption processes in diamond

In the diamond crystal structure, each carbon atom is neighbored by four other carbon atoms in a tetrahedral arrangement, as shown in Figure 3: other arrangements of carbon are possible and result in different materials such as amorphous carbon, graphite, etc. Each carbon atom has four outer electrons (the so-called *valence electrons*), and when the carbon atoms bond to each other in the diamond crystal there is an electron pair bond between each carbon atom pair: this sharing of electrons between nearest neighbors forms the archetypal *covalent bond*.

There are two ways in which this structure can absorb light:

- if the energy of the light is high enough, electrons can be knocked out of the bonds; this requires short wavelength light (ultraviolet)

- at long wavelengths (infrared), the absorbed light generates phonons, setting the carbon atoms into vibration
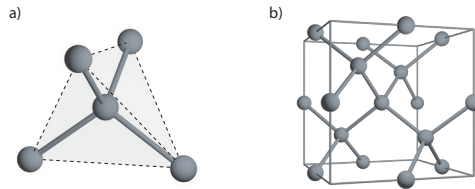
Figure 3. a) In diamond, each carbon atom is covalently bonded to its four nearest neighbors in a tetrahedral configuration: each bond is formed by the sharing of one of four valence electrons with a nearest neighbor. **b)** The diamond structure is frequently illustrated using the conventional unit cell, which provides greater context and displays a section of the lattice which is repeated throughout the entire crystal.

The absorption spectrum of a defect-free diamond for wavelengths between 0.2 and 20 μm (the visible region is between 0.4 and 0.7 μm) is given in Figure 4. At short wavelengths (around 0.23 μm) the ultraviolet light has sufficient energy to remove electrons from the electron-pair bonds, and at wavelengths shorter than this the diamond absorbs strongly, giving rise to the so-called *absorption edge*. In the infrared part of the spectrum, between 2.5 and 6.5 μm, there are the characteristic two- and three-phonon absorption bands at wavelengths where the infrared radiation can set the carbon atoms into vibration. For a defect-free diamond, as a result of its homonuclear tetrahedral symmetry, there is no one-phonon absorption (i.e., absorption of light which results in the creation of a single phonon, corresponding to the region with wavenumbers less than 1332 cm^{-1}, or equivalently wavelengths of greater than 7.5 μm).

The absorption edge, produced when a photon knocks out a valence electron from a bond, occurs at ~0.23 μm, corresponding to an energy of 5.49 eV. For a brief time that electron becomes available to conduct electricity, as it is no longer tightly bound to its original atom. It is useful to summarize this situation on an *energy level diagram* such as that shown in Figure 5. For a defect-free diamond in the dark, the valence band (comprised of the bonding, valence electrons, which are not free to move through the crystal) is completely filled with
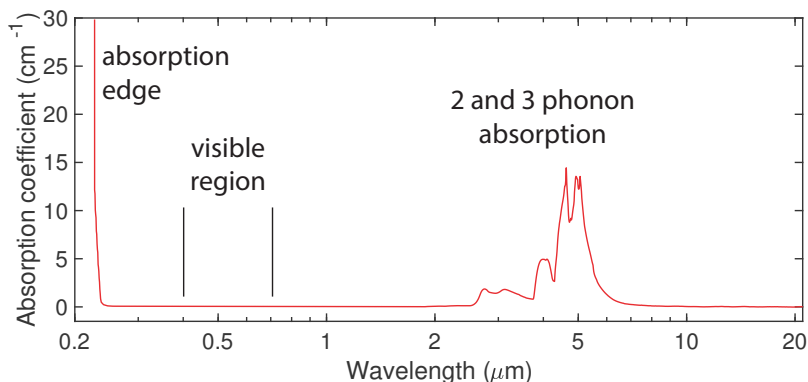
Figure 4. Aside from characteristic two- and three-phonon absorption in the mid-infrared, defect-free diamond is transparent from >20 μm to the band gap threshold at 225 nm (5.49 eV).
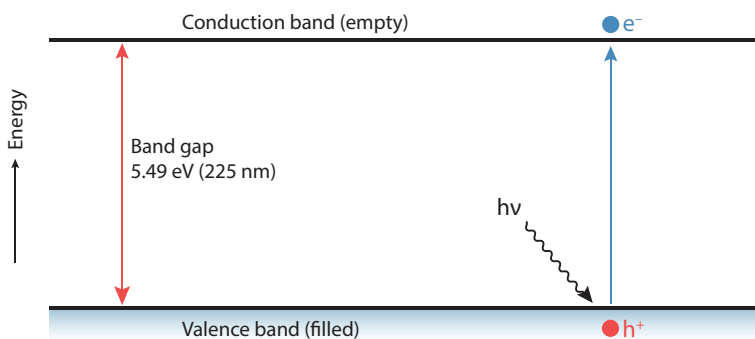

Figure 5. Energy level diagram for defect-free diamond. At room temperature and in the absence of light, all electrons reside in the valence band and participate in the covalent bonding of diamond. UV light of energy hν > 5.49 eV (< 225 nm) can excite valence band electrons (e⁻) into the conduction band, allowing them briefly to contribute to electrical conductivity within the diamond, and leaving behind a net positive charge (hole, h⁺) in the valence band.

electrons; consequently, the conduction band (which corresponds to high-energy states that do not participate in bonding and in which the electrons are instead free to move through the crystal) contains no electrons. The energy separation of the bands is 5.49 eV and is known as the *band gap*. Illuminating the diamond with ultraviolet light of wavelength shorter than 0.23 μm excites an electron from the valence band to the conduction band and leaves a *hole* in the valence band. This is a greatly simplified picture; nevertheless, it is useful in illustrating the processes behind some optical transitions. Note that it is also possible to *thermally* excite electrons from the valence to the conduction band; however, for this to occur, the available thermal energy $\sim k_B T$—where k_B is the Boltzmann constant and T is the temperature—must be at least comparable to the band gap, which only occurs in diamond for extreme temperatures well in excess of 1000 °C but is of crucial importance in other semiconductors such as silicon.

For a defect-free diamond there is no absorption in the visible region, and it is therefore completely colorless. In reality, most diamonds are colored, and so must absorb light in the visible region. This absorption is due to the presence of defects within the colored diamond: these defects and their associated effects are discussed from the next section onward.

Infrared absorption

Figure 6 shows the infrared spectrum of a defect-free (intrinsic) diamond recorded using a FTIR spectrometer. To retain a similar appearance to historical spectra (which generally used μm for the horizontal axis), most FTIR instruments plot the data with wavenumbers increasing from right to left, as shown here. As discussed above, defect-free diamond possesses no one-phonon absorption; however, there are processes which allow absorption involving combinations of two or more phonons. This characteristic absorption spectrum unmistakably identifies diamond. As the spectrum is intrinsic to diamond, it is also invaluable in the analysis of infrared spectra of diamond. The absorption coefficient of a 1 cm thick diamond is 12.3 cm^{-1} at 2000 cm^{-1} (Tang et al. 2005): this enables the conversion from absorbance to absorption coefficient to be made without measuring the path length through the diamond, which can be difficult in the case of gem-cut samples that are designed to produce multiple internal reflections.
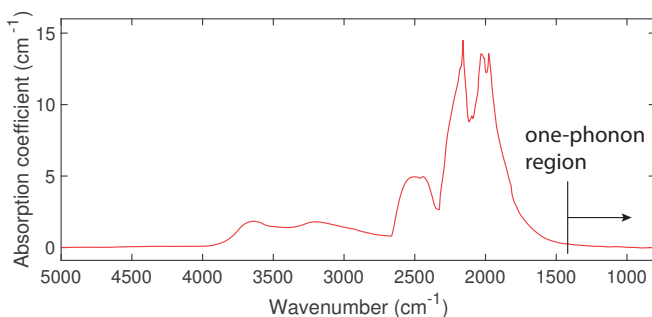
Figure 6. Infrared spectrum of intrinsic diamond, displaying the characteristic multi-phonon absorption at approximately 1500 cm^{-1} to 4000 cm^{-1}. The homonuclear tetrahedral symmetry of defect-free diamond means that bulk absorption processes which create only one phonon are not possible, yielding no absorption in the one-phonon region of 1332 cm^{-1} and below.

SPECTROSCOPY AND PROPERTIES OF IMPERFECT DIAMOND

Introduction

Defect-free diamond is an important physics playground and technological tool due to its well-known list of superlative properties, such as its hardness, thermal conductivity, transparency window and so on. However, for geological, gemological and quantum technology applications, it is the *flaws* within a diamond which are most important.

Defects in crystals can be classified into two broad categories: point defects and extended defects. Point defects encompass those defects which are "point-like", and which typically can be described within only one or two diamond unit cells, with fewer than ten atoms deviating significantly from the perfect, pure-carbon diamond structure. Extended defects include crystallographic faults such as dislocations and very large defect aggregates such as interstitial or vacancy clusters, and they may measure upwards of hundreds of microns in at least one dimension (a vacancy is simply a lattice site from which a carbon atom has been removed, leaving a vacant carbon site). It is essential to take both categories into account when determining the growth and subsequent history of a given diamond, and both are routinely employed in the discrimination between natural, synthetic, and treated diamond (see the final section below, and D'Haenens-Johansson et al. 2022, this volume).

This chapter is concerned primarily with the properties, treatment, and interaction of point defects in diamond. Most point defects in diamond are identified and studied through their interaction with light of various wavelengths. These interactions are defined by the geometrical, elemental and electronic structure of the defect in question and so are unique to a given defect, yielding a powerful spectroscopic "fingerprinting" tool.

Ultraviolet and visible absorption and luminescence

An absorption peak at 415 nm in diamond was first reported by Walter (1891). A more recent measurement of the absorption spectrum, which has a sharp line at 415 nm (violet) and a structured band that extends into the ultraviolet part of the spectrum and is commonly referred to as N3, is given in Figure 7. The line at 415 nm is much sharper at 77 K than it is at room temperature (293 K), and the structure in the band is also better defined at low temperature. When this absorption band is strong it gives the diamond a yellow color. Most of the perceived color is produced by a related absorption band known as N2 with its major peak at 478 nm (shown later in Fig. 32a).

Optical absorption in the visible range is the result of an electronic excitation, whereby an electron is "excited" to a higher energy state—analogous to a more energetic orbit in a hydrogen atom. These higher-energy electrons will attempt to lower their energy by a number of potential processes. For defects which absorb in the visible range, this frequently occurs by the subsequent emission of light, known generally as luminescence. Therefore, most colored diamonds will also luminesce under appropriate conditions.

Figure 8 shows a selection of uncut natural diamonds illuminated at 365 nm, many of which display a blue emission. An emission spectrum from one of the blue-luminescing diamonds is also given, and we see that there is a sharp line at 415 nm and a structured band at *longer* wavelengths (i.e., lower energy). It is clear that most of the band lies in the range 420 to 480 nm, which is why the luminescence appears blue.

Overlaying the absorption and luminescence spectra of N3 on a single diagram demonstrates that the spectra are approximately mirror images (Fig. 9). In order to understand this, the absorption transitions can be represented on an energy level diagram (Fig. 10). The sharp spectral line corresponds to an *electronic* transition from the ground state of the optical center to the excited state. If more energy is provided, the optical center and the surrounding lattice can also be set into vibration at certain characteristic frequencies. In luminescence the excited center can either relax directly to the ground state or, via vibrational levels, produce luminescence at lower energies. The ground and excited energy levels are located somewhere between the conduction band and the valence band (within the band gap). The energy separation of the ground and excited states can be measured with high precision, but in the majority of cases it is not possible (or very difficult) to determine their absolute positions in the band gap.
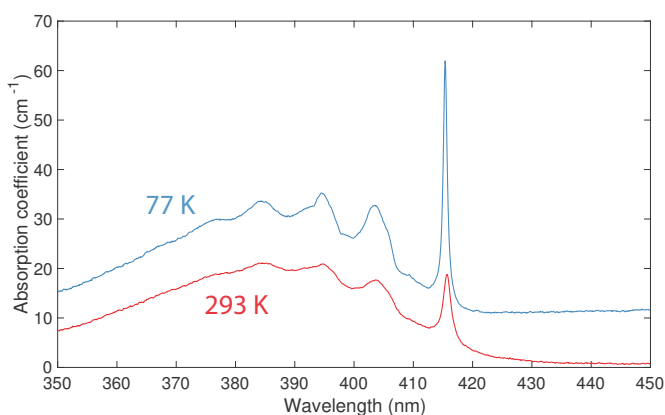
Figure 7. Optical absorption spectra of a diamond containing the 415 nm defect. The characteristic 415 nm peak and spectral sideband are better defined when the spectrum is collected with the sample at liquid nitrogen temperature (77 K) versus room temperature: this effect is typical of optically active point defects in diamond (and other materials). The spectra have been offset for clarity, and the total integrated absorption is the same at both temperatures.
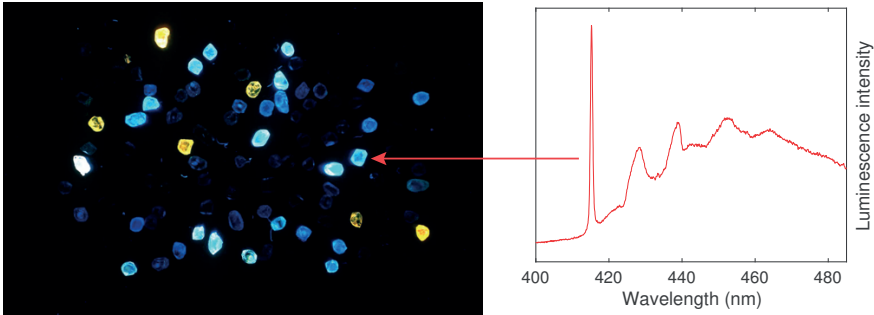
Figure 8. Visible luminescence of natural diamonds excited with 365 nm light. The light blue emission is due to the presence of the 415 nm (N3) defect, an exemplar liquid nitrogen temperature (~80 K) luminescence spectrum of which is given to the right.
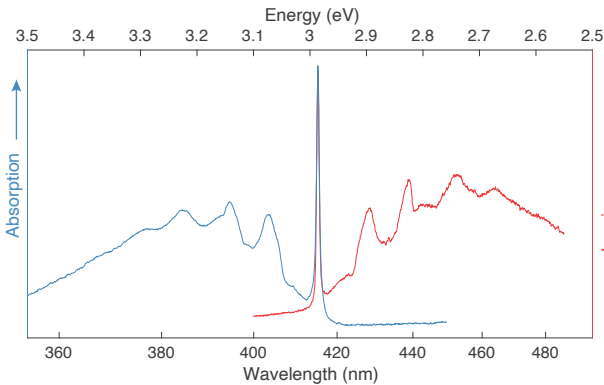

Figure 9. The characteristic luminescence and absorption spectra of the "415 nm (N3)" center at 80 K. When plotted on an energy scale (top), they are almost mirror images of one another.

The spectral structure of a point defect is a result of the electronic structure of the point defect and its interaction with the surrounding crystal. In an isolated atom or monatomic gas, optical transitions are very narrow in wavelength (energy) corresponding to well-defined electronic transitions between discrete electronic orbital states. Point defects in diamond are sometimes considered as trapped atoms or molecules: nevertheless, there is inevitably some interaction between the electronic structure of the point defect and the vibration continuum of the diamond lattice. This combination of interactions gives rise to so-called *vibronic* transitions, which involve both vibrational and electronic interactions.

Purely electronic transitions between the ground vibrational states of the ground and excited electronic states give rise to a spectral feature known as the zero-phonon line (ZPL). Optical spectra of point defects in diamond are often characterized by their ZPL wavelength, which is (typically) identical in absorption and emission. Vibronic transitions between the ground and excited electronic states involve the creation of lattice vibrations with characteristic energy $\hbar\Omega$ yielding a continuum of transitions which manifests as a broad, vibronic sideband. This sideband appears at higher energies than the ZPL in absorption, and lower energies than the ZPL in emission (Fig. 10).

Many defects in diamond have absorption and luminescence spectra similar to those shown in Figure 9 for the N3 center, though the particulars of a point defect's vibronic spectrum are a result of its electronic structure and coupling to vibrational modes. When identifying a particular optical vibronic spectrum, care must be exercised to compare both the ZPL wavelength and the
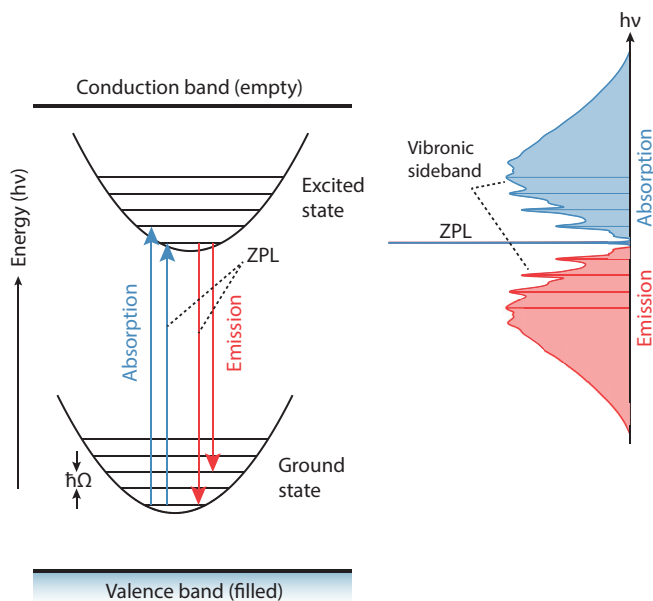
Figure 10. Illustration of a vibronic absorption and emission process at a point defect. Some point defects introduce additional electronic states into the band gap, giving rise to optical absorption in the UV, visible, or near-IR regions. If the energy (hv) of the incoming light is precisely the separation of the ground- and excited-states, then a sharp zero-phonon line (ZPL) is observed; if light of higher energy is incident on the defect then phonons are created in addition to the electronic excitation, causing the lattice to vibrate. When the defect subsequently relaxes, it emits light which is at the ZPL energy or lower. In both cases, the structure of the absorption / emission band is characteristic of the defect and related to the phonon energies ħΩ with which the defect interacts.

corresponding sideband to the reference spectrum, as multiple defects may emit at very similar wavelengths. For example, the unfortunately named H3 and 3H centers, with very similar ZPL wavelengths of 503.2 and 503.4 nm at 80 K, respectively, have different compositions but can be identified by their drastically different vibronic sidebands (Walker 1979).

Following excitation via the absorption of light, the time for which an optical center stays in the excited state covers a huge range, depending on the defect. In simple cases the time is determined by a statistical process rather similar to radioactivity. After the excitation is stopped, the luminescence decays exponentially with a characteristic decay time τ.

$$I(t) = I(0)e^{-\frac{t}{\tau}}$$

where $I(t)$ is the intensity at time t and $I(0)$ is the initial intensity. Luminescence decay times typically range from a few nanoseconds to 100s of microseconds. If there are no competing processes the measured decay time is equal to the true luminescence decay time of the optical center. However, there are often non-radiative transitions which make the measured decay time shorter and also decrease the luminescence efficiency; the luminescence is then said to have been *quenched* (see *Generation of luminescence*).

With a few exceptions, almost all the luminescence observed from diamond originates from vibronic bands, and there are quite literally several hundred ZPLs documented in the literature (Zaitsev 2001; Dischler 2012): several of the most important are detailed later in this chapter. In early studies it was fashionable to give a name (such as GR1, H3 or N3, where GR, H, and N indicated general radiation, heated, and natural, respectively) to an optical center,

depending on its origin (Clark et al. 1956a,b). With optical centers studied more recently it is conventional to refer either to the atomic structure, or the wavelength or energy of the ZPL. (However, atomic structures have been established for a relatively small number of optical centers in diamond, compared to the plethora of identified optical signatures.) Most optical centers in diamond can occur in both the neutral and negative charge states—for example, the nitrogen-vacancy center NV^0 and NV^-, where V indicates vacancy henceforth. To understand this, we consider a model that is used for *donors* and *acceptors* in semiconductors.

Donors, acceptors, and charge transfer

The best-studied donor in diamond is substitutional nitrogen (Fig. 11a), where substitutional indicates that the nitrogen atom remains approximately on the original carbon lattice site. Nitrogen is from group 5 of the periodic table and is trivalent in diamond: in its neutral charge state, three of its valence electrons are used for bonding as with the group 4 carbon atoms. The remaining two valence electrons form a lone pair that does not form a bond with the remaining carbon, leading to a distortion where this unique carbon and the nitrogen relax away from one another (Fig. 11a). It is much easier to remove one electron from this lone pair than it is to remove an electron from one of the bonds (i.e., it requires less energy), and if this happens, the nitrogen relaxes back to undistorted lattice site and the nitrogen is said to have *donated* an electron to the conduction band, leaving behind a positively charged substitutional nitrogen atom. On an energy-level diagram (Fig. 12) we show the nitrogen donor at 1.7 eV below the conduction band. Its position in the band gap has been determined by measuring, as a function of temperature (available thermal energy), the electrical conductivity of a diamond rich in substitutional nitrogen (Farrer 1969). When another defect is also present, the negative charge on the nitrogen atom may be transferred to that defect (see below).

Optical transitions are allowed from the donor level to the conduction band, but, because of additional restrictions, the threshold energy of 2.2 eV for optical absorption is higher than that determined by temperature-dependent electrical measurements. The 2.2 eV threshold is in the middle of the visible region at approximately 560 nm, and substitutional nitrogen's optical absorption ramps from this wavelength into the blue (Fig. 11b), producing a yellow color. This absorption structure is typical of electronic transitions between a defect and the conduction or valence band, where a continuum of band states leads to a broad, relatively featureless band. Contrast this spectrum to that of the 415 nm vibronic band which can also produce a yellow color (Fig. 7). Natural diamonds containing isolated substitutional N are rare (~0.1%; Dyer et al. 1965), but most diamond produced by high pressure high temperature (HPHT) synthesis contains nitrogen in this form.

A similar picture is used for substitutional boron in diamond (Fig. 11c). Boron is in group 3 of the periodic table and has only 3 valence electrons—one too few to complete diamond's 4-fold covalent bonding. It is conventional to refer to that missing electron as a *hole*, and under the influence of an electric field this hole moves as though it has a positive charge. Removing the hole is equivalent to the boron atom *accepting* an electron, and on an energy level diagram (Fig. 12) the boron *acceptor* lies 0.37 eV above the valence band, as determined by temperature-dependent electrical conductivity measurements (Collins and Williams 1971).

For boron, the ionization energy (the energy required to remove the positive hole) measured optically is the same as that determined from electrical conductivity measurements (Collins et al. 1969). In the absorption spectrum (Fig. 11d), at energies below the ionization energy, we see absorption due to transitions to internal excited states, followed by a continuum absorption at higher energy corresponding to photoionization of the hole. The spectrum shown is in the infrared region, but the continuum absorption extends into the visible region, giving the diamond a blue color. Natural diamonds containing boron as the major impurity are also rare, but it is not difficult to grow blue synthetic HPHT diamonds by removing nitrogen from the growth capsule and introducing ("doping with") boron.
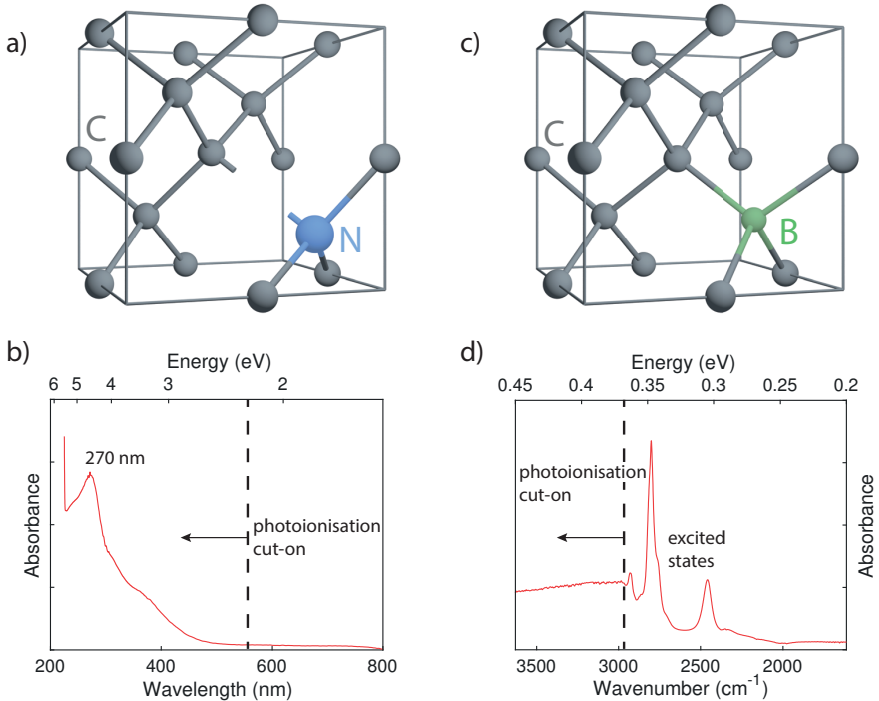
Figure 11. a) The structure of neutral substitutional nitrogen in diamond. Whereas carbon possesses four valence electrons (one for each nearest neighbor), the group-5 nitrogen atom possesses five, leaving an additional electron to be accommodated into one of its bonds, raising the bond energy and lengthening it to approximately 130% of a normal C–C bond (Etmimi et al. 2009). Incomplete bonds between atoms indicate that the atoms do not form a bond, and are included simply to provide a guide to the eye. **b)** It is possible to optically ionize neutral substitutional nitrogen with light of $\lambda < 560$ nm, leading to its characteristic optical absorption spectrum and associated 270 nm absorption peak (Jones et al. 2009). **c)** Boron, belonging to periodic group 3, possesses one fewer valence electron than carbon and therefore it is energetically favorable for it to accept one: this results in one bond contracting slightly (to approximately 98% of a normal C–C bond; Goss and Briddon 2006). **d)** Approximately 0.37 eV is required to thermally or optically excite an electron from the valence band to the acceptor state of substitutional boron. Boron's photoionization continuum extends into the visible region, lending a blue color to the diamond. Note that the intrinsic diamond absorption has been subtracted from this spectrum.
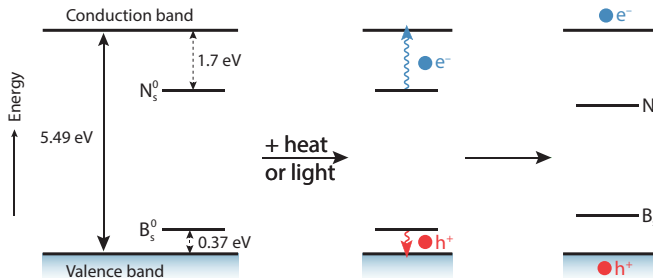
Figure 12. Illustration of the donor and acceptor processes for substitutional nitrogen and boron, the neutral charge states of which lie relatively close to the conduction and valence bands, respectively. The addition of sufficient heat or light can excite an electron from the nitrogen to the conduction band, resulting in an electron in the conduction band and a positively charged defect: the same is true for the boron, with hole, boron, valence, and negatively in place of electron, nitrogen, conduction, and positively, respectively. The charge carrier is then free to migrate through the band, potentially to be trapped by another point defect.

In diamonds with a high single-nitrogen (N_s) concentration, the negative charge state of a given defect—such as NV—is typically dominant, whereas the neutral charge state is more prominent in diamonds with a low single-nitrogen concentration (Collins 2002). The interpretation here is that when a neutral defect center (X^0) and a neutral substitutional nitrogen defect (N_s^0) are in close proximity, the nitrogen can donate an electron, converting the defect to its negatively charged version and leaving the nitrogen in a positive charge state:

$$X^0 + N_s^0 \leftrightarrow X^- + N_s^+$$
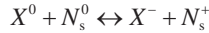
This effect is known as *charge transfer*, and the defect *X* can be considered as a *charge trap*. In many cases it is possible to drive the reverse process, ionizing X^- and reverting back to the neutral charge states of the relevant defects: however, the particulars of the charge transfer process, and the extent to which it can be driven in either direction, are sample- and defect-specific. In extreme cases this can lead to significant visible color changes which can be driven by light (photochromism) or heat (thermochromism) (Fig. 13): natural diamonds which exhibit photochromism are sometimes referred to as chameleon (Hainschwang et al. 2005). These changes are typically reversible as they do not involve the creation or destruction of defect centers, but only the migration of charge between charge traps: the processes are therefore distinct from high-temperature annealing, which involves the migration, creation, and destruction of defect centers. The only defect center which has been definitively identified as positively charged in diamonds containing B as the major impurity is the positively charged substitutional nitrogen center, N_s^+ (Lawson et al. 1998).

### Generation of luminescence

There are several distinct ways in which luminescence can be generated in diamond. All of the following excitation mechanisms have been reported—we will focus our discussion on the first two as the most common and of practical significance in diamond:

- Photoluminescence (photon beam)

- Cathodoluminescence (electron beam)

- Electroluminescence (current injection)

- Ionoluminescence (ion beam)

- Thermoluminescence (heat)

- Triboluminescence (friction / polishing)

Some diamonds may also emit light for milliseconds to tens of seconds after the excitation is shut off—a phenomenon known as phosphorescence.

Below-band gap photoluminescence. In photoluminescence (PL) with below-band gap excitation (i.e., using light of <5.49 eV), a vibronic optical center is excited using a wavelength lying within its absorption band, directly exciting an internal transition within the defect; after a short time, the center relaxes to the ground state, emitting light in the luminescence sideband (see Fig. 10). For this process to occur, the incident light (for spectroscopy, typically a laser beam) must lie within the absorption band of the defect center (Fig. 14). Excitation using wavelengths outside the defect's absorption band will not induce photoluminescence from that center, enabling selective excitation of defects. This can be a powerful tool in characterizing samples which contain multiple defects whose spectra overlap.

The physical mechanisms behind the PL and Raman processes are distinct; however, they are experimentally measured in the same way. Therefore, care should be taken to ensure that spectral features are correctly ascribed to luminescence or Raman. Raman shift is relative to the
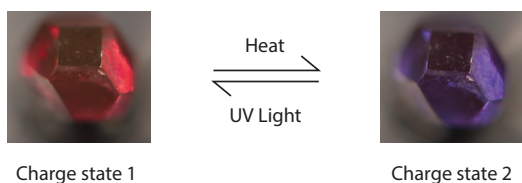
Figure 13. An extreme example of photo- and thermo-chromism. The HPHT-grown sample contains N_2V and NV defects in abundance. By driving charge between substitutional nitrogen and these defects, it is possible to bias towards N_2V^0 and NV^0 giving a red hue (**left**); or N_2V^- and NV^- yielding a purple color. Adapted from Dale (2015).
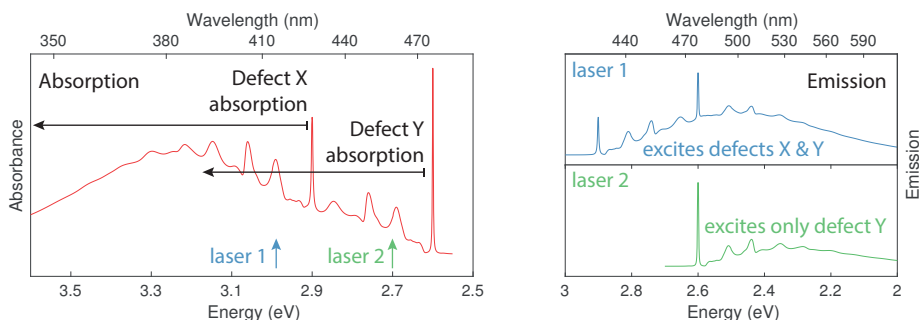
Figure 14. An absorption measurement (**left**) measures the total absorption of the sample at a given wavelength. Where the absorption profiles of multiple defects overlap, the absorbance at that wavelength is the sum of the absorption due to all defects simultaneously. In this example, the absorbance at 3.0 eV is a result of absorption by both X & Y defects, while at 2.7 eV only defect Y contributes to the spectrum. Using sub-band gap excitation, photoluminescence can be excited from multiple defect centers selectively. A sub-band gap laser incident on a crystal containing multiple defects will only induce photoluminescence from those centers which absorb it. Using laser 1 (3.0 eV), both defects X & Y will absorb the laser light and subsequently emit (**top right**); using laser 2 (2.7 eV), only defect Y will absorb and emit (**bottom right**).

excitation wavelength, and spectral features arising from a Raman process will always manifest at the same energy shift from the excitation energy. Photoluminescence ZPL energies are a property of the emitting defect and are fixed in absolute energy. We therefore distinguish between Raman and PL by measuring the same area of the crystal using different energy excitations and comparing spectral features plotted against energy shift from the excitation energy.

Photoluminescence can be quenched in diamonds with high concentrations of defects, because of non-radiative energy transfer between defect centers following optical excitation (Davies and Crossfield 1973; Crossfield et al. 1974). The quenching defects do not themselves necessarily luminesce: for example, substitutional nitrogen (PL-inactive) quenches PL from NV^- centers (Manson et al. 2018). Photoluminescence is therefore NOT a quantitative method for measuring defect concentrations. However, in diamonds with low concentrations of defects, a semi-quantitative estimate of defect concentrations can be made by comparing the intensity of the PL with the intensity of the Raman spectrum (or, in the case of a high-sensitivity instrument measuring a diamond which contains very low defect densities, by directly counting the defects—see *Quantification of defect concentrations*). Significant care must be taken when using a polarized light source such as a laser, as the intensity of the Raman line can change by over 100× depending on the crystallographic face being probed (Solin and Ramdas 1970; Grimsditch et al. 1978; Steele et al. 2016).

We note that the charge state in which a defect is measured can be sensitive to the laser wavelength used to excite it, in addition to the absorption-based considerations described above. For example, 532 nm is efficient at photoionizing NV^0 to produce NV^-, while 560 nm is not, and therefore the measured charge ratio $NV^0:NV^-$ is highly sensitive to the laser wavelength used to perform the measurement (Aslam et al. 2013).

The strengths of PL as a diagnostic and spectroscopic tool include its speed, relative insensitivity to surface contaminants, and production of spectra with sharp peaks which enable precise and potentially automatic analysis. By moving the sample under the laser beam (or rastering the laser beam itself), it is possible to map the relative concentrations of defects (Fig. 15), which can be important in understanding the incorporation mechanisms of defects or even aid in origin identification.

Cathodoluminescence. Electron-beam excitation, using electrons of energy typically 5 to 50 keV, excites electrons from the valence band to the conduction band, leaving holes in the valence band and producing electron–hole pairs. Penetration depths of the electron beam are ~0.2 μm at 5 keV and ~15 μm at 50 keV (Davies 1979). After excitation the electron and hole capture each other and form a short-lived center called an exciton, with a hydrogenic-like energy structure. In very pure diamond the electron and hole then annihilate, producing free-exciton recombination, which will not concern us here. In defect-containing diamond the excitons may be captured by optical centers which themselves become excited and then decay, producing characteristic luminescence—see the simplified schematic in Figure 16.

Cathodoluminescence (CL) images can be produced using a scanning electron microscope (SEM) or simply with a suitable electron gun. In the SEM an image can be produced by measuring the light generated by the electron beam via a detector which produces a signal proportional to the incident intensity. By synchronizing the data collection with the raster scan a digital map can be generated in which each pixel represents the intensity at that point. This information can be processed to produce a gray-scale image or a false color image. If the CL is passed through filters or a monochromator before reaching the detector, images can be produced which show the intensity distributions in different wavelength regions (a hyperspectral image).

An optical image can be obtained directly by photographing the specimen (using film or a digital camera) as it is scanned by the electron beam. Alternatively, a stationary defocused electron beam can be used to illuminate the full area of the specimen, from which a photographic image can be produced. This technique was used by Sumida and Lang (1981) in their seminal study of dislocation networks in natural Type IIb diamond. For less demanding applications the whole area of the specimen can be excited with a simple electron gun. The specimen may then be examined and photographed using an optical microscope placed above the viewing window (Henry 2020). An example of this technique is given in Figure 17, which is a photograph of a slice of natural diamond being irradiated with a defocused electron beam produced by a cold-cathode electron gun of the type described by Henry (2020). The mainly blue luminescence shows evidence of a complex growth history, and we can also see yellow/green CL originating from lines of plastic deformation. High magnification reveals patches of yellow luminescence from extended defects known as *giant platelets*. Using suitable collection optics, the spectra of these defects can be determined (Wight et al. 1971; Collins and Woods 1982). Many diamonds exhibit "Band A" CL, but there are, in fact, several different bands, and the CL may be blue or green. Much of the luminescence in Figure 17 originated from the blue band A.

Typical voltages encountered in an SEM are not high enough to directly induce lattice damage in diamond. For an electron beam focused to a small spot the excitation densities can be very high, ~10^{23} electron–hole pairs per cubic centimeter per second. The luminescence decay time of many optical centers in diamond is very short (typically 10 to 50 ns), and so even very small concentrations of such defects can produce bright cathodoluminescence, because each optical center can be excited and decay 10^7 to 10^8 times per second. However, some defect centers are not efficiently excited by an electron beam, even though they may have a short lifetime. CL from the negative NV center, for example, is exceedingly weak as a result of its charge dynamics, with emission instead via the neutral NV center as a result of electron-beam-induced charge conversion (Fedyanin and Agio 2016). Just like photoluminescence, CL is also quenched by high concentrations of defects (typically nitrogen-related).
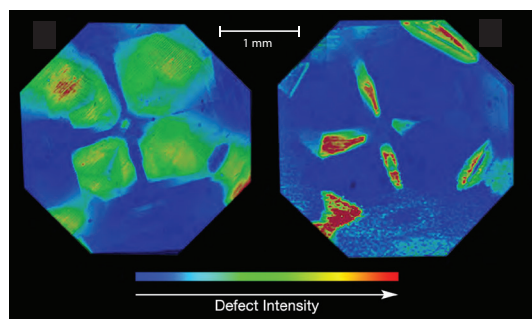
Figure 15. Mapping the intensity of spectral luminescence peaks by PL reveals the relative incorporation of point defects (637 nm, NV^- [**left**]; and 815 nm [**right**]) into different growth sectors of an HPHT-grown sample which was subsequently irradiated. Map collected from the table of a facetted gem. Modified from Loudin (2017).
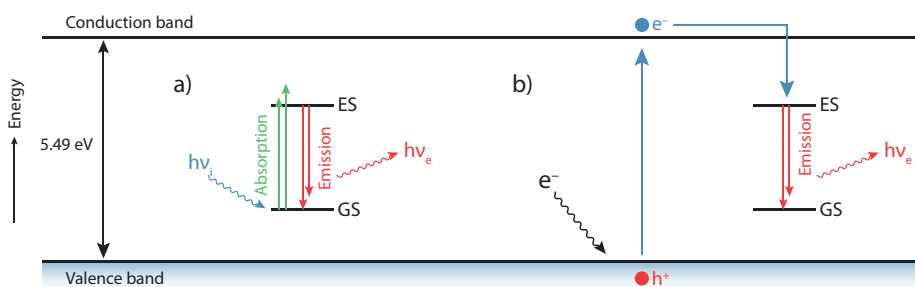
Figure 16. a) For below-band gap photoluminescence, the energy of the incoming photon (hv_i) is enough to excite an electron from a defect's ground state (GS) to its excited state (ES): the defect subsequently emits a lower-energy photon (hv_e). **b)** For cathodoluminescence, a high-energy electron excites an electron to the conduction band. The electron is then trapped by the excited state of a defect which subsequently emits.
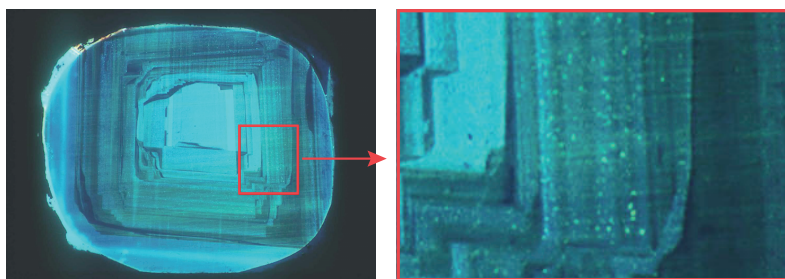
Figure 17. Growth horizons of a natural diamond as imaged by cathodoluminescence: the growth habit of the crystal at different times can be determined by the structure within the horizons. The blue emission is largely due to a broad band centered at approximately 435 nm known as "band A". High magnification (right) reveals the presence of yellow emission from giant platelets. Modified from Collins and Woods (1982).

As diamond is an effective electrical insulator, the incident electron beam in CL can induce local surface charging: to mitigate this charging, the diamond is typically coated in a thin conductive layer (frequently gold) before measurement. Due to this additional experimental complexity over PL, CL is less routinely employed in gemological and geological surveys.

Above-band gap photoluminescence. Electron–hole pairs may also be produced in diamond by the absorption of electromagnetic radiation with energy greater than the band gap. This is schematically similar to the process given in Figure 16b, with the incident electron being replaced by an ultraviolet photon with wavelength 225 nm or lower. The resulting luminescence is similar to that produced by electron excitation (Fig. 16b). The DiamondView instrument developed by the Diamond Trading Company (now De Beers Group Technologies) uses this technique. Figure 18 shows an image of a faceted CVD diamond excited in the DiamondView. The luminescence is produced by small concentrations of nitrogen-vacancy (NV) centers, and features striations which indicate the differential production of NV centers on different crystallographic surfaces during growth.

Finally, in this section we note that caution is required in comparing luminescence spectra from different publications. The "true" spectrum $L(\lambda)$ is measured with a spectrometer which has a response function $R(\lambda)$. The measured signal is therefore $L(\lambda) \times R(\lambda)$. The $R(\lambda)$ varies from spectrometer to spectrometer (for example, due to the use of different detection cameras). In principle, $R(\lambda)$ can be determined using a calibrated source (such as a tungsten lamp) but most published spectra are uncorrected.

Phosphorescence

Fluorescence and phosphorescence are two names given to luminescence, based on their decay times relative to typical human perception. Fluorescence is the name given to luminescence which decays effectively instantly on human timescales once the excitation source is removed, while phosphorescence is the name given to luminescence which persists for human-perceivable timescales after the excitation source is removed. As such, phosphorescence describes an empirical phenomenon rather than an underlying mechanism. Phosphorescence may arise from several distinct mechanisms, including internal transitions within a particular defect; and thermal trapping or release of charge carriers and their subsequent recombination (Dean 1965).

The most common phosphorescence spectra observed in diamond are related to donor-acceptor pair recombination, typically in conjunction with the presence of boron as a shallow acceptor. As a result, phosphorescence is routinely observed from both natural and synthetic semiconducting diamond with bands centered at approximately 500 and 660 nm (Walsh et al. 1971; Klein et al. 1995; Watanabe et al. 1997; Eaton-Magaña and Lu 2011). HPHT-grown near-colorless diamond, which often contains donors (nitrogen) and acceptors (boron) at the level of approximately 0.001–0.1 ppm, may also phosphoresce via this mechanism (D'Haenens-Johansson et al. 2015; Eaton-Magaña et al. 2017). Some features in synthetic diamond, such as the 499 nm system, may have internal electronic structure which results in intrinsic delayed luminescence (Khong et al. 1994; Wassell et al. 2018).

Phosphorescence spectra (example given in Fig. 19) are typically excited using near- or above-band gap excitation to generate large, transient concentrations of electron–hole pairs; however, it is possible to generate phosphorescence in some samples even with mid-gap energies (Freitas et al. 1994). Phosphorescence is routinely employed in the discrimination between natural and synthetic diamond (D'Haenens-Johansson et al. 2022, this volume), and several instruments have been built which specifically exploit this property.

Infrared absorption

As stated previously, defect-free diamond exhibits no absorption in the infrared one-phonon region. The addition of defects destroys the perfect symmetry of the diamond lattice, and some absorption is then created in the one-phonon region. As an example, Figure 20 shows the IR spectrum of a Type IaA diamond—one which contains most of the nitrogen in the form
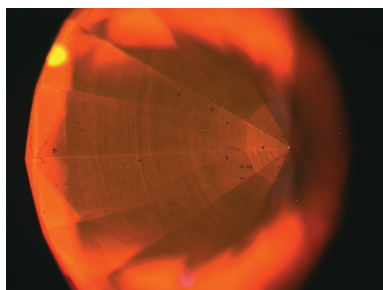
Figure 18. Typical DiamondView image of a synthetic diamond grown by chemical vapor deposition. The general orange color is the result of emission from nitrogen-vacancy (NV) defects. The striations are a result of differential production of NV defects on different crystallographic surfaces during growth.
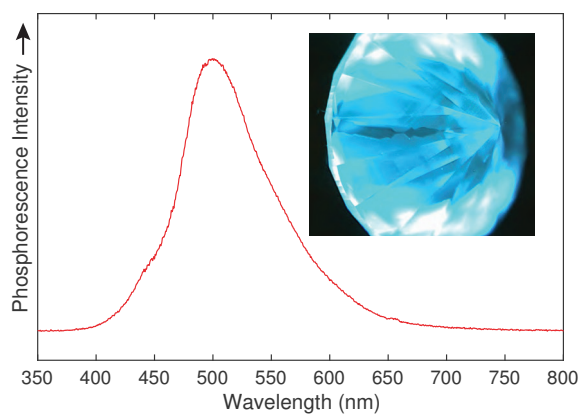
Figure 19. Typical phosphorescence spectrum from a near-colorless HPHT diamond. Inset: image of typical phosphorescence from a near-colorless HPHT-grown diamond. The difference in intensity is a combination of differential impurity uptake in different growth sectors (e.g., the dark line across the center) and the cut of the sample itself. Modified from D'Haenens-Johansson et al. (2015).
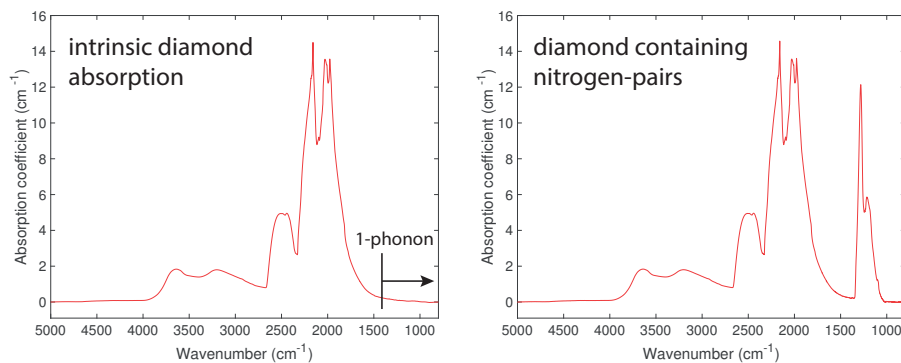
Figure 20. Infrared spectra of intrinsic diamond (**left**) and a diamond which contains a substantial quantity of defects in the form of nearest-neighbor nitrogen pairs. The nitrogen-pair defect is one of the most common found in natural diamond and is known as the A center.

of nearest-neighbor nitrogen pairs, known as *A centers* and with the atomic structure N_2. Note that the two neighboring nitrogen atoms in an A center do not chemically bond (and therefore do not represent a trapped diatomic nitrogen molecule): N_2 is employed henceforth on this understanding.

It has been shown by several researchers that there is a good correlation between the absorption coefficient at the peak of the one-phonon band (at 1282 cm^{-1}) and the concentration of A centers. Similar correlations have been established for the B aggregate of nitrogen (known as B centers, atomic structure N_4V, see *Aggregated nitrogen* later in this chapter) and for isolated substitutional nitrogen (often called the C center). These calibration factors enable the determination of the concentration of nitrogen in diamond, and the form in which it is present. This illustrates the power of optical absorption spectroscopy applied to diamond. In addition to quantifying nitrogen aggregates, IR absorption provides indispensable insight into many other defects and impurities, most notably hydrogen.

Electron paramagnetic resonance

It is important to note that while visible or infrared luminescence is an indication of the presence of structural or chemical defects, their absence does not imply a defect-free crystal. A particular defect may possess characteristic optical absorption or luminescence, or it may be entirely optically inactive, in which case we must turn to alternative techniques to assess a defect's presence and concentration. Optical phenomena such as absorption and emission of visible light in diamond are associated with the interaction between the *electric* field of an electromagnetic wave and electronic dipoles within the material. It is also possible for the material to interact with the *magnetic* component of an electromagnetic wave via magnetic dipoles.

Pure, crystallographically perfect diamond essentially does not interact with an external magnetic field, making it *non-magnetic*. However, defects within diamond are often *paramagnetic*, which means that they have intrinsic magnetic fields which align with an external magnetic field, enhancing it. This effect is due to an interaction between the external magnetic field and an electron's intrinsic magnetic moment, known as spin, within the defect. Spin can be visualized as a miniature bar magnet or compass needle, centered on the electron in question and possessing both a north and south pole.

Whether or not a particular defect is paramagnetic is dependent on its electronic configuration. Each defect electron is considered to contribute a spin which can either be "up" (+½) or "down" (-½): the overall spin of a defect, S, is the sum of these contributions over all local electrons. Defects with $S \geq ½$ are paramagnetic, and defects with $S = 0$ are non-magnetic. Therefore, defects with an odd number of electrons are always paramagnetic; defects with an even number of unpaired electrons are paramagnetic if the unpaired electrons' spin axes align, and non-magnetic if the unpaired electrons' spin axes are anti-aligned (Fig. 21).

The spin states of a paramagnetic defect will split into a total of $2S + 1$ energy levels in the presence of an external magnetic field (the Zeeman effect). Magnetic dipole transitions can be driven between these states using electromagnetic radiation of the correct energy—typically in the microwave region for moderate magnetic fields. By monitoring the absorption of a monochromatic microwave field and sweeping an external magnetic field, a spectrum of absorption against magnetic field strength can be generated. This form of spectroscopy is known as electron paramagnetic resonance (EPR) or electron spin resonance (ESR).

Unpaired electrons are incredibly sensitive to their local environment, and it is this property which gives EPR its spectroscopic power. For example, many chemical isotopes possess an intrinsic magnetic moment (nuclear spin) which interacts with the unpaired electron, giving an unambiguous fingerprint of that element's presence within the defect structure (Fig. 22) when combined with contextual information such as known impurities within the sample and their
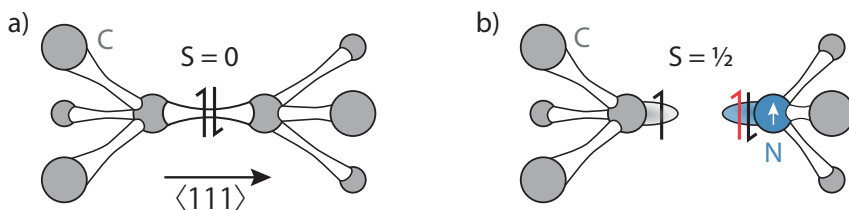
Figure 21. a) In defect-free diamond, each carbon atom possesses four valence electrons, and pairs each electron with one from each of its nearest neighbors, forming diamond's strong covalent bonds each of which has total spin $S=0$ and therefore is EPR-inactive. **b)** In neutrally charged substitutional nitrogen, the nitrogen and one of its nearest-neighbor carbon atoms do not bond, and the additional valence electron of the nitrogen has no pair from its nearest neighbors, resulting in overall spin $S=\frac{1}{2}$ and a measurable EPR signal. The nitrogen atom itself also has a small intrinsic magnetic moment (known as nuclear spin), as indicated by the white arrow.
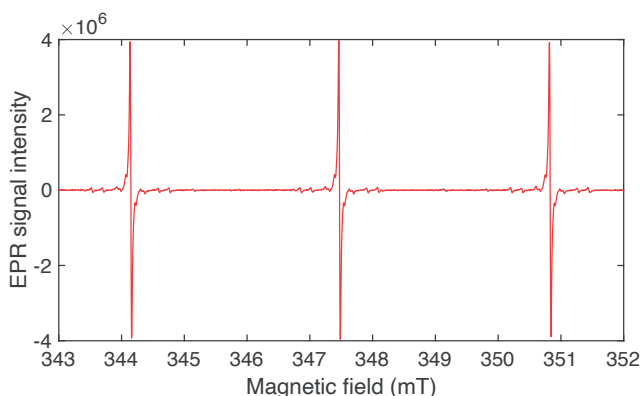
Figure 22. Typical EPR spectrum of a diamond containing neutrally charged substitutional nitrogen, N_s^0, with the magnetic field parallel to the <001> crystal axis. The three most intense lines are a result of magnetic interactions between the defect's unpaired electron spin and the nuclear spin of ^{14}N. The other, smaller "satellite" lines surrounding each primary transition are a result of further interactions with nearby ^{13}C nuclei (within a few angstroms). The magnetic field position and intensity of each satellite identifies the atomic location occupied by each corresponding ^{13}C, demonstrating the power of EPR spectroscopy (Cox et al. 1994; Peaker et al. 2016).

corresponding relative isotopic abundances. Thus, EPR allows the identification of previously unidentified magnetic spectra directly with their corresponding defect's chemical constituents and geometric configuration (and even neighboring defects): this approach can be particularly powerful for defect identification when combined with modern modeling techniques such as density functional theory (DFT) (Breeze et al. 2020). Additionally, the measured EPR spectrum depends on the relative orientation of the defect's symmetry axis and the external field. By measuring the EPR spectrum as a function of sample angle, an EPR spectrum can therefore yield information on a defect's symmetry, chemical constituents and electronic structure.

In addition to EPR's role in defect structure determination, it is also highly sensitive, non-destructive, and absolutely quantitative. Substitutional nitrogen concentrations down to 1 ppb can be routinely measured even in small (<0.5 ct) samples. The primary drawback of EPR as a spectroscopic tool is the requirement for the presence of unpaired spin, and as such it is most useful when employed in conjunction with traditional forms of optical spectroscopy for a holistic view of a given sample: this is particularly true in cases where the EPR spectrum of a defect has been reported but not its optical analogue, and hence EPR is required to identify the presence of the defect. In some particular cases it is possible to access an EPR-active ($S>0$) state of an otherwise EPR-inactive ($S=0$) defect via e.g., the application of appropriate optical illumination during the measurement (Felton et al. 2008).

EPR of diamond has a rich history within physics and has been instrumental in the identification and quantification of diamond point defects (Smith et al. 1959; Davies et al. 1978; Loubser and van Wyk 1978; van Wyk and Loubser 1993; Baker and Newton 1994; Newton 1994; van Wyk and Woods 1995; Nadolinny et al. 2017; Breeze et al. 2020). It has not been employed as a routine discrimination technique in gem labs due to the significant measurement timescales and the high operator skill required. Nevertheless, recent gemological publications have begun to adopt it to better understand both synthetic and natural diamond gemstones and their provenance (Wang et al. 2012).

Quantification of defect concentrations

Quantification of defect concentration is possible by several different techniques. As discussed previously, routine absolute quantification of defect concentrations is difficult to impossible in bulk using luminescence techniques. Unexpectedly, it is relatively simple to employ PL to quantify particular defects once their concentration is below approximately 1 μm^{-3}. With very high-sensitivity microscopes and single-photon-counting detectors it is possible to spectrally identify, and map, each emitting defect individually. This can be employed to study growth processes, defect diffusion and aggregation kinetics on a truly microscopic level (Chakravarthi et al. 2020), with resolutions of several hundred nanometers typically achieved (Fig. 23). However, for routine quantification absorption techniques must be employed, namely UV–Visible absorption (typically at liquid nitrogen temperature), IR absorption, and EPR spectroscopies.

For optical techniques, the measurement of absorption coefficient is not sufficient to absolutely quantify the defect concentration: identical concentrations of different defects will yield different absorption coefficients in a measurement, i.e., some defects absorb more of the incoming light *per defect* than others—a quantity known as the *absorption cross-section*. Accurately computing the absorption cross-section of a defect from first principles is nontrivial and would nevertheless require experimental verification.

To relate the concentration of a defect to its integrated optical absorption, we require a *calibration constant*. This constant enables us to measure the optical spectrum of a defect in a standard measurement and compute a defect density (in number per normalized volume). Here, we turn to other techniques for aid. For example, EPR is quantitative because one electron in defect A will absorb the same amount of energy as one electron in defect B. Therefore, by having a suitably well-characterized reference sample of known concentration, it is possible to quantify the concentration of other EPR-active defects. In cases where EPR-active defects have a known optical analogue, the concentration as measured by EPR can be related to the defect's integrated optical absorption, yielding a linear plot of concentration vs. integrated absorption, the gradient of which is the calibration constant for that defect. This approach using EPR is just one example of the ways in which optical absorption may be correlated with the corresponding defect concentration. In general, the integrated intensity of a sharp line, or the peak intensity of a broad band, is compared with a defect concentration measured by EPR, or nuclear activation analysis, or burning followed by residual gas analysis, or another suitable technique. For a vibronic band it is better to use the ZPL, rather than the peak intensity of the band, because the former is less susceptible to errors in determining the zero of absorption. A number of calibration constants for common defects are given in Davies (1999) and Dale (2015).

A research grade UV–Vis spectrophotometer will achieve a noise floor of approximately 0.001 A, which corresponds to approximately 0.2% transmission noise. Using NV^- as an exemplar defect in diamond which absorbs in the visible region: this corresponds to detection limits of approximately 0.1 and 1 ppb for diamonds which are 1 cm and 0.1 cm thick, respectively. EPR detection limits are on the order of 10^{12} spins, or approximately 0.1 ppb for a 1 ct diamond.
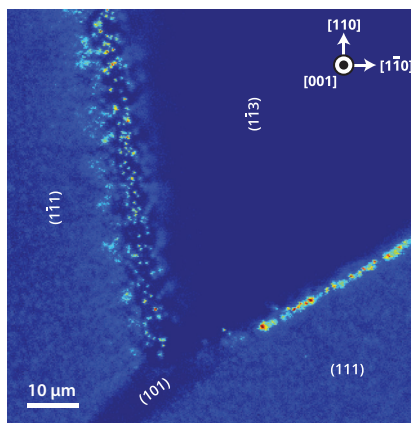
Figure 23. Decoration of growth sector boundaries in an as-grown HPHT sample, as imaged by a single-photon counting fluorescence microscope. The interfaces between each of the labelled growth sectors are decorated with isolated nitrogen-vacancy centers. Each of the bright spots on the $(1\bar{1}1) \rightarrow (1\bar{1}3)$ transition corresponds to a single atomic nitrogen-vacancy pair, which can be detected with high efficiency using an advanced fluorescence microscope. In this case it is possible to routinely reach ultimate sensitivity i.e., the detection of a single defect. The less bright fluorescence from the {111} planes arises from nickel uptake during growth in the {111} sectors, but not {110} or {113}. Modified from Diggle et al. (2020).

THE CLASSIFICATION OF DIAMOND

The classification scheme of diamond was largely developed between 1934 and 1986 and is based on the behavior in diamond of the two elements on either side of carbon in the periodic table—namely nitrogen and boron. The scheme is convenient for allocating a given diamond to a particular group with certain gross attributes, but there will be properties of that diamond that are not described by the classification scheme. In addition, there are some diamonds which cannot adequately be categorized by this scheme. A number of these exceptions will be described after the basic scheme has been outlined.

Nitrogen

Nitrogen is the dominant impurity in the majority of natural diamonds. Diamonds which contain sufficient nitrogen to produce easily measurable nitrogen-related absorption in the defect-induced one-phonon IR region are generically known as *Type I*. Other diamonds are generically known as *Type II*. It is important to recognize that a diamond classified as Type II may, nevertheless, contain small concentrations of nitrogen—"electronic grade" synthetic Type IIa CVD-grown diamond is typically specified as $[N_s^0]$ <5 ppb, which is undetectable by standard IR spectrometers, but routinely measurable using EPR (Cann 2009).

Nitrogen may be present as isolated substitutional atoms or in aggregated forms. Experiments carried out in the laboratory on the aggregation of nitrogen have played a crucial part in appreciating how these processes occur in nature. Nitrogen is believed to be incorporated in natural diamond initially on isolated substitutional sites. Natural diamonds which contain nitrogen of this type are rare (<0.1% of natural gem diamond; Smit et al. 2016), but nitrogen in high-pressure, high-temperature (HPHT) synthetic diamond is almost exclusively in this form. If present in sufficient concentration the substitutional nitrogen produces a characteristic absorption in the one-phonon region, shown in Figure 24. The major features are a broad band with a maximum at about 1130 cm^{-1}, and a sharp line at 1344 cm^{-1} associated with a *localized vibrational mode*. This description is used because the frequency is above the bulk lattice phonon maximum frequency of 1332 cm^{-1} and the vibration is therefore physically localized at the defect. This effect also accounts for the peak's narrow width. By measuring the absorption

coefficient at either of these locations the concentration of isolated substitutional nitrogen can be determined (Woods et al. 1990b; Lawson et al. 1998). The single nitrogen also produces absorption in the visible and ultraviolet spectral regions which gives the diamond a yellow color. Diamonds that contain isolated nitrogen in their absorption spectra are known as *Type Ib*.
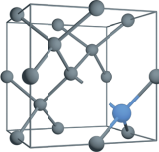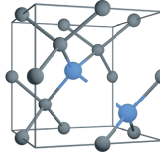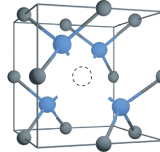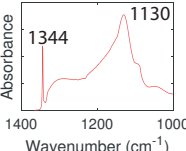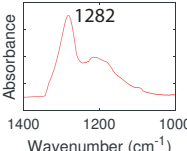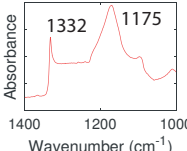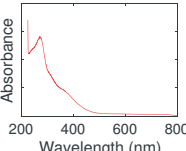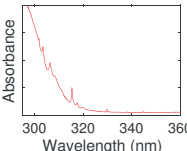
Aggregated nitrogen

After residing at geological temperatures over a billion-year timescale, most of the nitrogen in diamonds is present in aggregated forms. During the first stage of aggregation the A *center* is formed. Otherwise defect-free diamonds in which all the nitrogen is present as A centers have no absorption in the visible region (and so are colorless) but do exhibit characteristic absorption in the ultraviolet region (Fig. 24). A centers consist of two nearest-neighbor substitutional nitrogen atoms (Davies 1976). Diamonds containing aggregated nitrogen are known collectively as *Type Ia* and when most of the nitrogen is present as A centers the description *Type IaA* is used.

The one-phonon absorption for a Type IaA diamond is given in Figure 24. Nitrogen concentrations can be determined from the absorption coefficient in this region (usually measured at the most intense peak at 1282 cm^{-1}—see Woods et al. 1990a) and are typically 1000 ppm or higher. We see that nature has been very kind to the gem trade; if this concentration of nitrogen were present in the isolated substitutional form the diamonds would have a very unattractive deep yellow/brown color. However, as noted above, many Type IaA diamonds are colorless.

During the second stage of aggregation the B *center* is formed, and samples which have most of the nitrogen in this form are called *Type IaB* diamonds. The most intense peak in the one-phonon region is at approximately 1175 cm^{-1}. Studies of the B center indicate that it is comprised of 4 nitrogen atoms surrounding a vacancy (Loubser and van Wyk 1981). Near-surface carbon atoms may diffuse to the surface; in the bulk, they may diffuse to internal surfaces (voids) or become interstitial atoms. In the majority of Type IaB diamonds these carbon interstitials come together (perhaps with some nitrogen atoms) to form extended planar defects called *platelets* (Goss et al. 2003). Absorption at these platelets produces a moderately sharp peak in the region of 1365 cm^{-1}, frequently known as the *B' peak*, or simply the *platelet peak* (Woods 1986) (Fig. 25). In what are termed *regular diamonds* the intensity of the B' peak is proportional to the intensity of the absorption produced by the B centers. In the remaining (*irregular*) Type IaB diamonds the intensity of the B' peak is less than expected from this proportionality or may be completely absent (Woods 1986) as in Figure 24. Analysis of irregular diamonds demonstrates a lower concentration of platelets, which themselves possess typically smaller dimensions than those found in regular diamonds. This disparity is interpreted as platelet degradation and is understood to be indicative of higher mantle storage temperatures allowing its use as a mantle thermometer (Speich et al. 2018).

There is some weak absorption in the one-phonon region, called the *D band*, which is associated with the platelet peak, and this must be taken into account when the concentrations of the A and B centers are being calculated from the infrared spectra. Nitrogen concentrations in Type IaB diamond can be determined from the absorption coefficient due to B centers in the one-phonon region (usually measured at the plateau at 1282 cm^{-1}—see Woods et al. 1990a). Woods (1986) shows data for Type IaB diamonds with nitrogen concentrations up to 2000 ppm, but in most Type IaB diamonds the nitrogen concentration is lower.

The B center does not cause any known absorption in the ultraviolet or visible regions. However, diamonds containing B centers generally have absorption due to the N3 center. The N3 defect has three nitrogen atoms on a {111} plane, surrounding a common vacancy, N_3V^0 (i.e., a B center with one fewer nitrogen atoms). Woods (1986) showed that in regular Type IaB diamonds the intensity of the N3 absorption is proportional to the concentration of platelets. In such diamonds the platelet concentration is also proportional to the concentration of B centers,

Name	C center	A center	B center
Type	Ib	IaA	IaB
Form	N_s^0	N_2^0	N_4V^0
Structure			

| One-phonon spectrum | | | |

| UV-Vis spectrum | | | None from the B center. See text for details. |

Figure 24. Summary of the nitrogen-related defects which form the basis for the Type I diamond classification. Diamonds which contain a similar concentration of both A and B centers are referred to as Type IaAB or simply Type Ia. Incomplete bonds between atoms indicate that the atoms do not form a bond and are included simply to provide a guide to the eye.
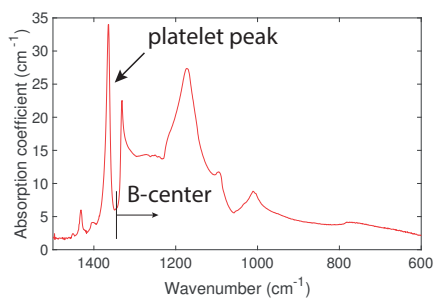
Figure 25. Infrared absorption spectrum of a regular Type IaB diamond, displaying a prominent B′ platelet peak at 1365 cm^{-1}.

and therefore Woods concluded that N3 centers are correlated with the absorption produced by B centers and that they are formed in a minor side reaction during the production of these B centers. That implies that the intensity of the N3 absorption is proportional to the intensity of the absorption produced by B centers in both regular and irregular Type IaB diamonds, though no systematic study has been carried out.

The nitrogen defects have been discussed separately, but most natural Type Ia diamonds contain a mixture of the A and B forms of nitrogen. These are normally described as *Type IaAB*, or simply *Type Ia*. Additionally, many natural diamonds containing C centers are better classified as Type Ib-IaA (Smit et al. 2016; Lai et al. 2019).

Boron

In a very small fraction of natural diamonds (approximately 0.1% (King et al. 1998) and less than 0.02% of gem quality diamonds (Smith et al. 2018)), substitutional boron is the major detectable impurity. These are *Type IIb* diamonds, and, as illustrated in Figure 11, such diamonds have an optical absorption with a continuum absorption starting at an energy of 0.37 eV in the infrared and extending into the red visible region: this is an electronic absorption corresponding to excitation of electrons from the valence band which are captured by the boron defect. In favorable cases this absorption gives the diamond an attractive light- to dark-blue color. Boron also produces some vibrational absorption in the defect-induced one-phonon region.

The ionization energy of boron is sufficiently low that about 1% can be thermally excited at room temperature, producing positive holes in the valence band (see Fig. 12). Type IIb diamond is therefore a *p-type semiconductor*—a semiconductor in which the majority charge carrier is holes (if electrons are the dominant carrier then the material is known as an *n-type semiconductor*). Wedepohl (1957) carried out Hall effect studies on Type IIb diamond and showed that, in order to explain the results satisfactorily, the diamonds must also contain donors at a smaller concentration than the concentration of boron acceptors. It is probable that this donor is nitrogen in the majority of natural diamonds.

The concentration of neutral boron acceptors $[B^0]$ is equal to the total boron concentration minus the donor concentration and can be determined (Collins and Williams 1971) from the area of the excited-state absorption peak at 0.348 eV (2802 cm^{-1}, Fig. 11d). Other regions of the absorption spectrum can also be used if the absorption at 0.348 eV is too strong (Howell et al. 2019). Boron is a widespread element in the Earth's crust with relatively low abundance, and it is probable that many diamonds contain boron. However, it is only those diamonds for which boron is the major impurity which are semiconductors and referred to as Type IIb. Those Type II diamonds which are not semiconductors are known as *Type IIa*. Recent evidence suggests that Type IIb diamonds originate deep within the Earth's mantle, beneath the transition zone (Smith et al. 2018).

Summary

The information given in this section is summarized in Figure 26. It is important to note that the type system does not capture many important properties: the color of a sample may change between many hues without changing type, as the type system does not capture information on visible properties. This means that many nitrogen-containing defects such as 3107 cm^{-1} (see later section on *Hydrogen*), and defects which do not present recognized IR absorption spectra, such as NV and N$_3$V, are not considered by the type system, and a diamond which presents no nitrogen-related features in its one-phonon absorption spectrum may nevertheless contain easily detectable concentrations of nitrogen in other forms. Additionally, many diamonds have absorption bands in the one-phonon region that are not included in this scheme. For example, a broad absorption and corresponding sharp peak at 1332 cm^{-1} has been shown by Lawson et al. (1998) to arise at positively charged single nitrogen, N$_s^+$. Hainschwang et al. (2012) found that many natural diamonds, classified as Type Ib because of the presence of absorption at 1344 cm^{-1}, have an additional "Y component" in the one-phonon absorption, with a maximum at 1145 cm^{-1}. Collins and Mohammed (1982) showed that, for all the samples in their study of natural brown diamonds which have an absorption band at 480 nm, the one-phonon region also has an absorption peak at 1240 cm^{-1} that is not seen in other diamonds. Finally, there is a whole range of absorption spectra associated with other impurities (such as hydrogen, nickel etc.) which are not captured by the type system.
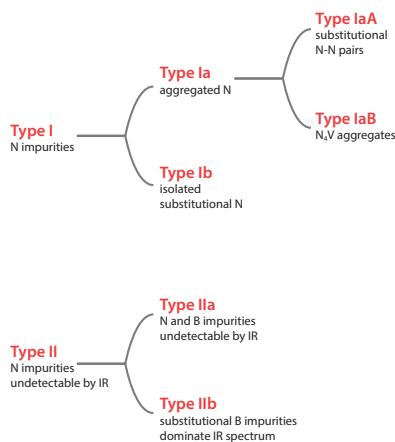
Figure 26. Summary of diamond type classification system, which is based on the absence or presence of infrared absorption due to specific forms of boron and nitrogen incorporated into the diamond. The type system can provide a gross idea of sample properties in the majority of natural samples, but by no means does it fully describe a given sample's attributes. As an example, it is possible to modify a sample's color from brown to green to pink without changing its type.

POINT DEFECTS IN DIAMOND

Defects are ubiquitous in both natural and synthetic diamond and give rise to many of the properties that make diamond such an extraordinary material technologically, gemologically and geologically. Even the most extraordinary Type IIa colorless natural diamond contains a significant concentration of defects, though not in a configuration that produces color. Having established the methods by which point defects in diamond are typically analyzed, and discussed the type system, which allows gross classification of diamonds into groups, we now discuss several important point defects and their properties directly. Defect interactions and their macroscopic effects on a crystal are summarized in the subsequent sections.

Intrinsic

Intrinsic point defects are those defects which involve carbon as the only element (i.e., no impurities). The most important of these are the vacancy and the interstitial—a vacant lattice site and a carbon atom off-site, respectively. These defects are the primary result of irradiation of diamond, whether by electrons, gamma rays or other particle sources: incoming radiation imparts enough energy locally to break the carbon–carbon bonds, displacing the atom to an off-site position and leaving behind a vacant lattice site (Fig. 27).
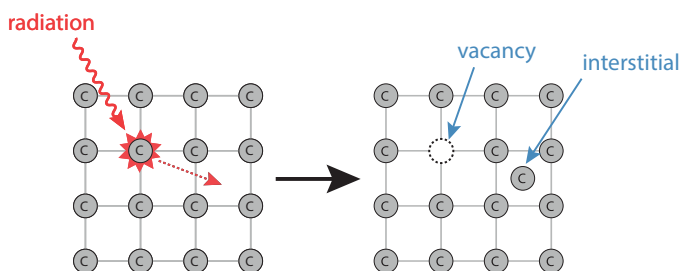
Figure 27. Intrinsic damage created by high energy radiation (electrons, gamma rays, ions etc.). The vacancy-interstitial pair may immediately self-annihilate or may freeze in, whereupon subsequent heating will allow them to diffuse separately through the lattice.

If the vacancy and interstitial do not self-annihilate during the irradiation, they are "frozen" into the lattice. The concentrations of vacancies and interstitials may not be equal, and their ratio depends on the sample temperature during irradiation, with lower concentrations of interstitials being detected for irradiation performed at higher temperature (Newton et al. 2002). This apparent discrepancy has been attributed to charge-related effects during the irradiation itself, which produces transient, high-mobility, interstitials which can subsequently combine with other defects or impurities to form defect complexes, or annihilate at internal or external surfaces (Newton et al. 2002). In the absence of irradiation, interstitials are mobile at relatively low temperatures of ≥400 °C (Iakoubovskii et al. 2003), at which point a small proportion (~30%) of vacancies are also lost, presumably to vacancy–interstitial recombination (Allers et al. 1998). Vacancies themselves begin to diffuse at approximately 700 °C (Davies et al. 1992; Newton et al. 2002). These (lab-timescale) threshold temperatures are frequently encountered in the defect investigations and in color treatments, as the migration and subsequent combination of vacancies and interstitials with other defects can drastically modify a diamond's properties (see *Treatments to change the color of diamond*).

Spectroscopically, the neutral and negatively charged vacancy possess ZPLs at 741 and 394 nm and are referred to as GR1 and ND1, respectively: the ratio between them is typically controlled by the substitutional nitrogen concentration (see *Donors, acceptors, and charge transfer*). There are several configurations of intrinsic interstitial, but the most common gives rise to a weak absorption at approximately 667 nm (Smith et al. 2004). Other optically-active configurations such as TR12 and 3H are less-well characterized and typically estimated to be significantly lower in concentration (Walker 1977; Davies 1981). Both the common interstitial (Twitchen et al. 1996) and the negatively-charged vacancy (Twitchen et al. 1999) can also be studied by EPR.

Macroscopic stress within a diamond, caused by e.g., metallic inclusions or crystallographic faults, can be visualized using a microscope equipped with two linear polarizers, one either side of the sample and with their polarization axes mutually perpendicular (colloquially known as "crossed polarizers"). Under this configuration, stress-induced birefringence causes those areas of the crystal which are under stress to become bright, while unstressed regions remain dark. The vast majority of natural diamonds contain fibrous networks of dislocations (extended defects that can span macroscopic dimensions of a crystal) (Fig. 28). In natural Type II diamond, or very low nitrogen concentration Type I, the birefringence pattern often appears "cross-hatched" when viewed through crossed polarizers—a result of the random strains to which the crystal has been exposed during residence time in the mantle. For natural Type Ia diamonds with significant nitrogen impurities, mottled or linear patterns dominate the birefringence seen under crossed polarizers. Dislocation networks in Type II diamonds can often be visualized directly (rather than indirectly via their effect on crystal stress, as we observe in crossed polarizers) using DiamondView or cathodoluminescence (see Sumida and Lang 1981, Harris et al. 2022, this volume). In natural Type IIa samples, plastic deformations can yield an overall brown color due to absorption at vacancy clusters (Mäki et al. 2009, 2011), which can be subsequently removed by HPHT treatment (see *Brown diamonds*). In contrast, synthetic crystals frequently display dislocations which follow the growth direction (in the case of CVD) or the interfaces between growth sectors (in the case of HPHT), yielding characteristic patterns which are indicative of the crystal habit during growth

Nitrogen

As discussed in the previous section, nitrogen is present in significant quantities in the vast majority of natural diamond. For synthetics, atmospheric nitrogen is incorporated into HPHT-grown diamond in significant quantities (>100 ppm) unless specific chemical traps ("getters") are added to the synthesis capsule, which are often employed to target colorless Type IIa material with <0.1 ppm nitrogen. In CVD growth, the addition of even small amounts of nitrogen
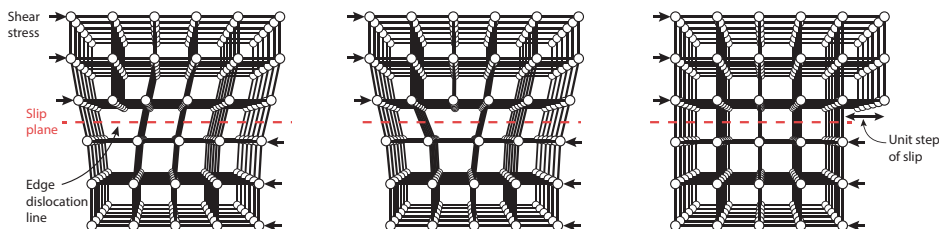
Figure 28. Example of an edge dislocation propagating through a crystal as a result of differential (shear) stresses. In diamond these dislocations do not anneal out at mantle temperatures, even over geological timescales. Adapted from Callister (2006).

(10–200 ppm) to the gas phase can increase the growth rate by 2–10× (Tallaire et al. 2006, 2013; Achard et al. 2007), with incorporation into the diamond typically <100× lower than the gas phase concentration. Therefore, the vast majority of colorless CVD gems contain <1 ppm nitrogen to achieve commercially viable growth rates while retaining relatively high color grades.

The aggregation of nitrogen from substitutional towards higher-order aggregates (N_2 and N_4V) forms the basis of the Type I classification system. The additional electron present in substitutional nitrogen (vs. carbon) introduces strain into the lattice, extending one of the N–C bonds by up to 30% (Breuer and Briddon 1996). The nitrogen aggregation process therefore achieves a reduction in lattice strain via the clustering of nitrogen atoms around a vacancy (or one another). The energy required to directly swap a nitrogen and carbon atom is extremely high, and thus nitrogen migration through the lattice is understood to be mediated by vacancies and interstitials (Collins 1980; Pinto et al. 2012; Jones et al. 2015) (Fig. 29).

At its simplest level, the aggregation of nitrogen from substitutional to the N_4V (B center) form can be expressed as

$$4N_s \rightarrow N_4V + C_I$$

where C_I is an interstitial carbon atom: large aggregates of interstitials form the platelets associated with high levels of nitrogen aggregation. The balance between aggregation termination and substitutional nitrogen (or other aggregates) is determined by temperature: lower temperatures drive towards higher aggregation while extreme temperatures are capable of destroying aggregates, re-producing substitutional nitrogen (Brozel et al. 1978; Evans and Qi 1982).

Chemical kinetics. The aggregation of nitrogen is typically described in terms of chemical reaction kinetics. Early, seminal work on nitrogen aggregation laid the foundations for the application of quantitative chemical kinetics to the study of defect production, migration and diffusion in diamond (Chrenko et al. 1977; Collins 1980; Allen and Evans 1981; Evans and Qi 1982). Almost universally, energy to drive an aggregation process in diamond is provided as heat by raising the temperature of the sample (though it is possible to perform "local" annealing via non-thermal-equilibrium methods, Chen et al. 2019).
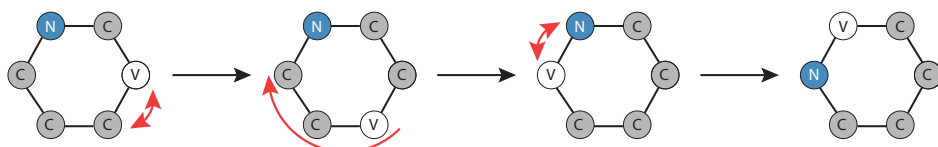
Figure 29. Vacancy-assisted migration of nitrogen in diamond. The direct carbon-nitrogen exchange process is extremely high in energy and is not expected to occur at any practicable temperature. Instead, the nitrogen moves by exchange with a vacancy, which becomes mobile at approximately 700 °C. It is possible for the same vacancy to be trapped and re-trapped, allowing the pseudo-NV to migrate through the lattice as a unit. Adapted from Pinto et al. (2012).

Chemical kinetics can occur with different qualitative behavior, with the relevant processes being described as "first-order", "second-order", or "mixed second-order". A first-order process simply requires enough energy for the chemical reaction to occur—sources and sinks are assumed to be infinite and the rate depends only on the remaining concentration. An example would be the destruction of a point defect (say, NV→ N + V). Within a first-order process, the change in concentration of the defect in question ([X]) is simply proportional to its concentration

$$\frac{d[X]}{dt} = -k[X]$$

The rate constant k depends exponentially on the ratio of the energy required to drive the process (its activation energy, E_A) to the available thermal energy ($k_B T$, where k_B is the Boltzmann constant and T the temperature in thermal equilibrium). The attempt frequency, f, describes the rate at which the constituents involved in the process encounter one another during random diffusion through the lattice:

$$k = f \exp\left(-\frac{E_A}{k_B T}\right) \tag{1}$$

A second-order process depends on the energy required for the process to occur, the energy available to drive the process, and the concentration of the reactants. Taking for example the aggregation of $2 N_S \rightarrow N_2$, the process will run quickly at first but slow down as the available reactants (N_S) decrease appreciably in concentration throughout the process. Mathematically, the change in concentration of the defect is now non-linear in concentration

$$\frac{d[X]}{dt} = -k[X]^2$$

A mixed second-order process is one in which the reactants are different—for instance, N + V → NV—in which case the process depends on the changing concentrations of both precursors,

$$\frac{d[X]}{dt} = \frac{d[Y]}{dt} = -k[X][Y]$$

Practically, the relevant chemical kinetics and their associated activation energies are determined in experiments where the same sample is heated multiple times at the same temperature and the concentrations of defects are measured at each interval (isothermal annealing), or by heating the same sample for the same time at multiple temperatures (isochronal annealing). A particular defect concentration may not straightforwardly fit any of the above descriptions if multiple, otherwise independent, processes are occurring simultaneously. The determination of the attempt frequency f in Equation (1) can be particularly difficult and often an attempt frequency matching the diamond lattice vibration frequency is assumed (though not necessarily always justified).

To illustrate the impact of different kinetic orders, we consider their behavior in different concentration regimes. A first-order process rate is independent of concentration, and as long as samples are held at the same temperature, the same percentage change in concentration will be observed for any non-zero starting concentration and a fixed annealing time. For second-order (and mixed second-order) processes, the percentage change will depend strongly on the starting concentrations, with higher concentrations yielding higher percentage changes. Therefore, the temperature at which a measurable change in concentration is observed will

differ between different samples. This insight, combined with careful measurement and reasoning, gives us a route to employ nitrogen aggregation to study a diamond's residence conditions over geological timescales (Allen and Evans 1981; Taylor et al. 1990, 1996; Bulanova 1995; Mendelssohn and Milledge 1995; Kohn et al. 2016; Speich et al. 2018)—see Nimis (2022, this volume) for further information.

Production of A and B centers. The aggregation of C centers to A centers in synthetic Type Ib material is found to obey second-order kinetics, with the production of N_2 (A centers) being second-order in the substitutional nitrogen (C center) concentration (Chrenko et al. 1977). Aggregation occurs on lab timescales at approximately ≥1700 °C; at 2400 °C the rate of production and destruction of A centers reaches equilibrium at approximately 95% in the A center form (Evans and Qi 1982; Collins et al. 2000). The rate of aggregation can be dramatically enhanced at low temperatures by first irradiating the material before thermal annealing, introducing vacancies and interstitials into the lattice and hence greatly increasing the mobility of nitrogen (as discussed previously) (Collins 1980; Allen and Evans 1981). Additionally, the aggregation rate is sensitive to the pressure during annealing, with higher pressure associated with decreased aggregation rates (Kiflawi et al. 1997).

Aggregation to N_4V (B centers) occurs at approximately ≥2400 °C on lab timescales. Precise evaluations of experiments become difficult in these conditions due to the extreme temperatures and pressures (typically >8 GPa). However, upon heating Type IaA diamond, the resulting B center concentration was found to be second-order in A centers, suggesting that it is A centers themselves which aggregate to form B centers. During this process little change is observed in the N_3V (N3) concentration, suggesting that it is a byproduct of aggregation, rather than necessarily the primary aggregation route (Brozel et al. 1978). Alternatively, it may be that the capture cross-section of N_3V for diffusing nitrogen (presumably in the NV or N_I form) is very high, making it difficult to generate high concentrations in the presence of other decomposing or diffusing nitrogen species (Kiflawi and Bruley 2000). The production of B centers is associated with the production of platelets, which initially were interpreted as large nitrogen-containing aggregates but which are now recognized as interstitial carbon aggregates (see previous subsection) (Woods 1986; Kiflawi et al. 1998; Goss et al. 2003).

Degradation of platelets in Type IaB diamond is associated directly with the formation of dislocation loops and the production of <111>-oriented crystalline structures called voidites, with diameters of approximately 2–200 nm (Hirsch et al. 1986; Evans et al. 1995; Navon et al. 2017), in addition to changes in size distribution and concentration of platelets (Kiflawi and Bruley 2000). The precise constituents of voidites are unclear, though there is evidence that they contain solid NH_3 (Rudloff-Grund et al. 2016) or crystalline molecular nitrogen under high pressure (Bruley and Brown 1989; Kiflawi and Bruley 2000; Navon et al. 2017), and they may therefore arise due to the release of nitrogen impurities trapped at platelets or due to decomposition of B centers themselves.

Diffusion, aggregation, and formation of nitrogen-related defects. While significant study has been dedicated to the aggregation and behavior of nitrogen in diamond, there are still some aspects which remain unclear. In material containing mainly single nitrogen and which is subsequently irradiated, the vacancy-assisted aggregation of N to N_2V is relatively well-understood: vacancies produced during irradiation diffuse to substitutional nitrogen at 700–800 °C, forming NV; the NV unit becomes mobile around ≥ 1400 °C, and diffuses to remaining substitutional nitrogen to form N_2V. This may capture an interstitial or emit a vacancy, forming A centers typically at ≥1800 °C. However, the subsequent formation routes for N_3V and N_4V remain under debate. As discussed above, the concentration of N_3V is typically low even in samples which eventually produce significant B centers (N_4V) at ≥ 2400 °C.

Irradiation of material which already contains aggregated nitrogen produces different defects. In irradiated Type IaA material, N_2V production occurs at much lower temperatures (~800 °C) via vacancy capture at the A centers themselves (Collins and Kiflawi 2009). Irradiation of Type IaB diamond, followed by annealing at ~ 800 °C, leads to the formation of $N_4V_2^0$, a color center known as H4, via vacancy capture at B centers (Loubser and van Wyk 1981).

Nitrogen itself is an efficient trap for interstitials as well as vacancies. Carbon interstitials which diffuse to substitutional nitrogen are understood to become nitrogen interstitials (Kiflawi and Mainwood 1996). These nitrogen interstitials are mobile at relatively low temperatures (~600 °C, Liggins et al. 2010) and may themselves capture another nitrogen to become the di-nitrogen interstitial, which is responsible for the infrared H1a absorption at 1450 cm^{-1} (Liggins et al. 2010). The temperature at which carbon interstitial capture occurs is type-dependent (Woods 1984; Fisher and Lawson 1998), but H1a typically anneals out at 1400–1500 °C (Liggins et al. 2010).

In natural diamond it is assumed that nitrogen is incorporated substitutionally. It is unclear which mechanism mediates nitrogen aggregation from substitutional to A centers in the majority of natural diamond, but it is likely that both interstitial and vacancy-driven processes are involved. The spontaneous thermal formation energies for interstitials and vacancies are both much higher than their migration energies (Jones et al. 2015), so that if they are introduced to the diamond by means other than direct thermal formation, they can assist with diffusion of atoms through the material at more moderate temperatures. Natural diamonds frequently include flaws (e.g., dislocations, damage from low-flux natural irradiation, material around inclusions) which can act as sources of vacancies and interstitials and it is likely that they provide the mechanism for early-stage aggregation in these diamonds.

Within the nitrogen-vacancy family, the most important color centers and their corresponding ZPLs are: $NV^{0/-}$ (575 / 637 nm); $N_2V^{0/-}$ (H3: 503 nm / H2: 986 nm); N_3V^0 (N3: 415 nm); $N_4V_2^0$ (H4: 496 nm). With the exception of N_3V^0, which is almost ubiquitous among Type Ia diamonds, these nitrogen-vacancy related centers are typically introduced during irradiation and annealing, though they can also be present in natural diamonds typically at low concentrations. An in-depth summary of nitrogen-related point defects and their interactions in diamond can be found in Ashfold et al. (2020), and their effect on diamond color is discussed in the following sections. Characteristic spectral features of dominant nitrogen-related defects are summarized in Table 1.
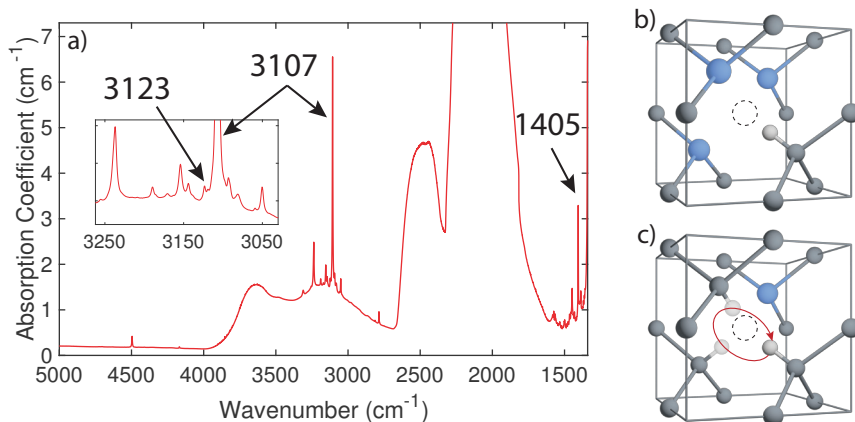
Hydrogen

Hydrogen is a common impurity in diamond, with some natural diamonds reported to contain in excess of 1000 ppm (Hudson and Tsong 1977). Hydrogen content in gem-quality single crystal synthetic diamond is typically much lower (<50 ppm). It is unclear where the majority of hydrogen resides: CVD diamond which is irradiated and subsequently annealed can produce high concentrations of NVH (Hartland 2014), suggesting a latent source of hydrogen which is as-yet unidentified. Hydrogen can be diffused into the diamond lattice under elevated temperature and pressure, resulting in the passivation of boron acceptors (Chevallier et al. 1998) and the destruction of NV centers by hydrogen capture (which become NVH) (Stacey et al. 2012), further providing evidence for the solubility of hydrogen without revealing its location.

The presence of (currently detectable) hydrogen in diamond is primarily monitored through the vibration of carbon–hydrogen (C–H) stretch modes, which occur at characteristically high frequencies (~2800–3300 cm^{-1}) in IR absorption spectra. Of these C–H modes, the most important is the 3107 cm^{-1} mode, which in so-called hydrogen-rich diamond can be stronger in peak intensity than the intrinsic multi-phonon absorption (Fritsch et al. 2007). This mode, and its corresponding 1405 cm^{-1} bend mode, were recently recognized as belonging to N_3VH^0— a defect which is identical to the N3 (N_3V^0) defect but with a hydrogen bonded to the single

Table 1. Summary of some common spectroscopic optical features encountered in diamond (where NIR and MIR denote near- and mid-infrared, respectively). For a more comprehensive review of spectroscopic features, their properties and origins, see the reviews by Zaitsev (2001) and Dischler (2012). LVM is Local Vibrational Mode (see *Ultraviolet and visible absorption and luminescence*).

Name	Structure	ZPL wavelength (nm)	Mid-IR features (cm^{-1})
		UV–Vis–NIR vibronic bands listed by ZPL wavelength	
ND1	V^-	394	
N3	N_3V_0	415	
H4	N_4V_{20}	496	
H3	N_2V_0	503	
	NV_0	575	
594 nm		594	
	NV^-	637	
	C_I	666 broad (absorption only)	
	SiV^-	737	
GR1	V_0	741	
	SiV_0	946	
H2	N_2V^-	986	
		Infrared LVMs and vibronic transitions	
H1c			5171 peak
H1b			4941 peak
H1a	N_{2I}		1450 peak
	N_3VH^0		1405, 3107 peaks
	B_s^0	Decreasing ramp from red to blue	2464, 2802; ramp. Weak one-phonon
		Infrared vibrational one-phonon absorption	
C center	N_s^0	Ramp from green to blue	1344 LVM; 1130 peak
	N_s^+		1332, 1046 peaks
B center	N_4V^0		1332, 1175 peaks
A center	N_2^0	UV ramp	1282 peak

carbon neighbor (Goss et al. 2014) (Fig. 30a,b). Studies of high-hydrogen, high-nitrogen CVD diamond have identified hydrogen-containing analogues of other nitrogen aggregates, including NVH^0 (3123 cm^{-1}, Cruddace 2007; Khan et al. 2013, 520 nm band, Khan et al. 2009) and NVH^- (EPR, Glover et al. 2003) (Fig. 30c), N_2VH^0 (EPR, Hartland 2014), and N_3VH^0 (1405 and 3107 cm^{-1}, Goss et al. 2014; Coxon et al. 2020). Of these, only N_3VH^0 has been definitively reported in natural diamond, though diamonds high in hydrogen often exhibit absorption at 3123 cm^{-1}, which is likely to correspond to low concentrations of NVH^0 (Fig. 30a,c). The N_4VH configuration is not expected to be energetically favorable, and therefore N_3VH^0 presumably represents the termination of this aggregation cycle over geological timescales. N_3VH^0 is stable to at least 2300 °C (Zaitsev et al. 2018).

Figure 30. a) Infrared spectrum of a high-hydrogen natural sample. The one phonon region has been omitted due to spectrometer saturation. A plethora of C–H modes at 3000–3300 cm^{-1} is evident, with the most intense being the 3107 cm^{-1} stretch mode associated with N_3VH^0: its corresponding bend mode at 1405 cm^{-1} and bend-stretch overtone at 4496 cm^{-1} are also typically observed in this material. Atomic structure of **b)** N_3VH^0 and **c)** $NVH^{0/-}$. The former is identical to the defect which produces N3 (415 nm) absorption, but with a hydrogen bonded to the lone carbon neighbor. In NVH, the hydrogen quantum-mechanically tunnels between the three equivalent carbon neighbors.

The presence of significant hydrogen in CVD-grown high-nitrogen material means that the aggregation of nitrogen in this material does not necessarily follow the route described in the previous subsection. Typically, both the standard nitrogen aggregates (N_nV, with $n = 1$–4) and their hydrogen-containing analogues (N_nVH, with $n = 1$–3) are produced simultaneously with the latter typically the dominant route (Zaitsev et al. 2018). As the hydrogen-containing analogues are not associated with strong color (except a weak pink induced by NVH), then similar colors to those obtained with HPHT-grown diamond may often be produced in CVD material, but with a lower efficiency in terms of starting nitrogen to target color. A complete understanding of annealing behavior and dominant aggregation mechanisms in this material is yet to be reached (Ashfold et al. 2020).

Many other C–H IR modes have been reported but in the vast majority of cases their atomic origin is unknown—summaries are given in Fritsch et al. (2007) and Meng et al. (2008). Analysis of these modes is complicated by the fact that they occur within a relatively narrow frequency window—an indication that the C–H frequency is only weakly perturbed by the atomic configuration of the corresponding defect. Therefore, direct assignment via theoretical modelling methods is difficult without supporting experimental evidence (e.g., isotopic shift or annealing behavior). Unlike nitrogen and many other elements, there are very few sharp absorption or emission lines which are associated with hydrogen-related defects.

Boron

Boron forms part of the diamond classification system as a result of its dramatic effect on diamond color. Despite its prominence within the diamond community, very few boron-related centers have been definitively identified. This is especially surprising given its high solubility in diamond, which allows boron incorporation up to 10%. At these concentrations, diamond becomes metallic (rather than semiconducting) and is even capable of superconductivity at low temperature (Ekimov et al. 2004). Its metallic behavior can be exploited in many electrochemical applications in conjunction with diamond's supreme chemical resistance (Macpherson 2015).

Several luminescence centers are associated with Type IIb diamond (e.g., 648 and 776 nm, Green 2013; Eaton-Magaña and Ardon 2016) but they are universally weak, having no effect on perceived color: corresponding absorption spectra of these samples typically show only broad absorption with no sharp features (King et al. 1998). Even intrinsic features such as neutral vacancies can be suppressed in Type IIb diamond following irradiation (Collins 1977; Green 2013). It seems likely that this is a result of the boron acting as an acceptor and biasing defects towards otherwise unattainable charge states; however, there is as-yet no convincing evidence for V^+, and the suppression of V^0 may instead be a result of boron-vacancy (or boron-interstitial) interactions.

Other elements

A huge number of defects have been identified in diamond, primarily through visible or infrared optical measurements and covering much of the periodic table (Zaitsev 2001; Dischler 2012). The intentional introduction of other elements into diamond has accelerated due to its potential in optically-active quantum computation, communication, and sensing technologies (Aharonovich and Neu 2014; Atatüre et al. 2018; Awschalom et al. 2018; Barry et al. 2020). This is typically performed either by doping during synthesis (Tallaire et al. 2015; Ekimov and Kondrin 2017; Achard et al. 2020) or by post-growth ion implantation (Pezzagna et al. 2011; Lühmann et al. 2018). As a result of the plethora of possible defects we make no attempt to be comprehensive and simply mention those elements which are most prominent.

Silicon is incredibly rare in natural diamond but common in CVD-grown synthetics, typically arising due to contaminants in the growth reactor. This typically results in ZPLs at 737 nm (which splits into a doublet at liquid nitrogen temperature) and 946 nm corresponding to SiV^- and SiV^0, respectively, and which can be visible in both luminescence and absorption (D'Haenens-Johansson et al. 2011). Unlike NV, where the nitrogen resides effectively in a carbon lattice site, in $SiV^{0/-}$ the silicon relaxes back towards the vacancy, adopting a so-called semi-vacancy position (Fig. 31a,b). At high SiV^0 concentrations, samples can become moderately gray–blue colored and be heavily photochromic (Breeze et al. 2020). Recent measurements have also identified substitutional silicon, which is detectable only as a broad peak around 1338 cm^{-1} in the infrared (Breeze et al. 2020).

A large number of transition-metal-related defects (predominantly nickel and cobalt) have also been identified, primarily as a result of their use as a solvent-catalyst during HPHT synthesis. Nickel-related defects are relatively frequently observed in natural diamond (though typically not in concentrations high enough to affect color; Breeding et al. 2018). Much of the work on transition metal defects has been completed using EPR (Baker and Newton 1994; Nadolinny and
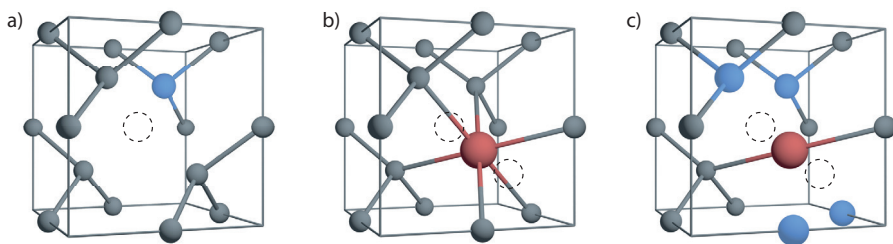
Figure 31. Comparison of the **a)** NV and **b)** SiV / NiV / CoV structures. In both cases, only one atom (by number) is missing from the lattice, but in NV the nitrogen remains substitutional, whereas for the larger atoms the impurity relaxes back to a bond-centered location between two lattice sites; the so-called semi-vacancy position. **c)** The NE8 defect, which emits at 794 nm, is comprised of a nickel atom in the semi-vacancy position with four of its nearest-neighbors replaced by nitrogen (Kupriyanov et al. 1999; Nadolinny et al. 2005).

Yelisseyev 1994; Nadolinny et al. 1999, 2005). Several well-known optical centers are related to nickel (e.g., the 494, 658, and 883/885 nm centers, Lawson and Kanda 1993; Yelisseyev and Kanda 2007; Breeding et al. 2018) and cobalt (Lawson et al. 1996; Kupriyanov et al. 2001) though in most cases their atomic configuration is not definitively known.

The presence of nickel or cobalt in Type Ib diamond (as would be expected for an HPHT crystal grown with a Ni or Co solvent) can significantly enhance nitrogen aggregation processes at lower temperatures via the efficient generation of highly-mobile nitrogen interstitials (Fisher and Lawson 1998; Nadolinny et al. 2000). It is also possible for the nickel itself to trap nitrogen atoms, producing defects such as NE8 (Fig. 31c). The uptake of nickel and cobalt during HPHT synthesis is sector-dependent (Fisher and Lawson 1998), with nickel-related optical activity detected only in the {111} sectors (Collins et al. 1990)—this can be revealed by luminescence mapping (Fig. 15, 23).

As of writing, color centers in diamond are attracting significant attention for quantum sensing, quantum computation, and quantum communication. The most-studied defect in this field is NV^- (see reviews at (Doherty et al. 2013; Rondin et al. 2014)), though other vacancy-containing defects (such as the group-IV-vacancies, $SiV^{0/-}$, GeV^-, SnV^- and PbV^-) are also attractive as a result of their much higher ZPL to sideband ratio, which is critical in many photonic applications (Aharonovich and Neu 2014; Atatüre et al. 2018; Bassett et al. 2019). Fundamentally, diamond is an ideal host for many of these defects as the vibrational and electronic coupling between the defect and the bulk lattice is often weak, allowing the defects themselves to be treated and manipulated as "trapped atoms": this is highly unusual among solid state defects, as in most materials the coupling between the defect and the material is large, leading to broad emission bands with weak ZPLs and poor electron spin lifetimes—critical metrics for their intended applications.

NATURALLY COLORED DIAMONDS

The variety of point defects and extended defects that can occur in diamond is vast, but only a few of those defects (the so-called color centers) give rise to the beautiful colors that make many gem diamonds so sought-after. Although most people think of colorless diamonds as the purest and most valuable gems, the occurrence of certain defects in diamond in just the right concentrations is so rare that stones with saturated red, orange, blue, and green hues have commanded sums of up to US $4M per carat (Associated Press 2015).

The geological history of a diamond also has an important impact on the color centers that are present. Some color-producing point defects like isolated substitutional nitrogen and boron are incorporated during crystallization and growth deep in the Earth's mantle. More complex color centers involving nitrogen are created during the aggregation process when the diamond resides for long time periods in the mantle under elevated temperatures and pressures. Many of the more common extended defects in diamond that produce color are thought to be created by differential stresses within the mantle, resulting in plastic deformation of the diamond lattice (Fig. 28). Finally, radiation-related color centers involving vacancies are often created in the diamond lattice in alluvial settings in the shallow crust where diamonds may soak in radioactive fluids for thousands of years (Breeding et al. 2018). A closer look at the causes of the most common colors in gem diamonds gives a better understanding of how these stones can inform a complex world of diamond geology.

Yellow diamonds

Yellow is one of the most common colors seen in gem diamond and can occur with a huge range in saturations from slight yellow to deeply saturated yellow, depending on the particular nitrogen color center present. In most pale to moderately colored yellow diamonds,

high concentrations of N3 defects, created by the nitrogen aggregation process during mantle residence, produce a series of absorptions in the visible range, ~415 nm (N3) as well as 451 nm, and 478 nm (N2), that give rise to a "straw yellow" color (Fig. 32a). These diamonds are collectively referred to in the gem industry as "Cape" diamonds due to their original association with South Africa, but they occur in nearly all diamond deposits (King et al. 2005). Much of the D to Z color grading system developed by GIA—where D is colorless and Z is light yellow—is a gradation in the concentration of Cape defects, and thus yellow color, in gem diamonds (King et al. 2008). With significant concentrations or in larger stones with longer optical pathlengths, Cape defects can produce strongly saturated yellow hues as well.

Some of the more intensely colored yellow diamonds, often known in the gem trade as "canary" yellows, owe their color to the presence of C centers that were incorporated at crystallization, though most canary yellow diamonds have undergone significant aggregation and occur as Type IaA diamonds with traces of isolated substitutional nitrogen. These isolated substitutional nitrogen atoms strongly absorb light in the ultraviolet to blue parts of the spectrum (Fig. 32b), to create deeply saturated yellow hues with relatively low concentrations of C centers present (a few tens of ppm). Due to the aggregation pathway that most nitrogen impurities in diamond follow, these strongly colored yellow Type Ib diamonds are very rare and are thought to be preserved by either very short residence times in the mantle or crystallization and residence in regions of unusually cold mantle (Smit et al. 2016). Those rare examples of nearly pure Type Ib diamond typically have very low total nitrogen concentrations. Nearly all yellow color produced in laboratory grown diamonds is also a result of C center absorption.
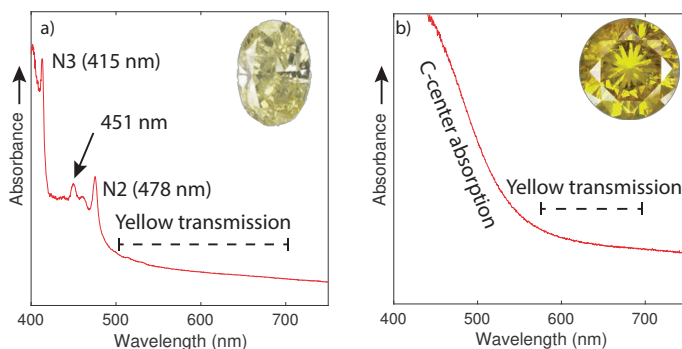
Figure 32. "Cape" diamonds show absorption features from N3 defects **(a)** while "canary" diamonds rely on substitutional nitrogen **(b)** to produce their characteristic yellow colors. Spectra collected with the samples at 80 K.

Other notable, but rare, causes of yellow color include the previously-discussed H3 defect, and 480 nm visible absorption band. The 480 nm visible absorption band is a poorly understood defect that is intimately associated with the presence of C centers, with theoretical modelling suggesting it could be oxygen-related (Gali et al. 2001). Orange colored diamonds are closely related to yellows and are primarily produced by 480 nm band absorption or by a combination of C centers and "Y components" (Hainschwang et al. 2012).

Brown diamonds

Brown is also one of the most common hues encountered in natural diamonds and, in conjunction with yellow, forms the basis for the D to Z color grading range (King et al. 2008). Unlike many other color centers involving complex point defects, brown color is thought to be a product of the extended defects produced by plastic deformation of the diamond lattice.

As planes of atoms are offset during deformation, clusters of up to 70 vacancies form (Fujita et al. 2009). Vacancy clusters absorb light across the visible range, increasing toward the ultraviolet, and produce varying shades of brown depending on their abundance (Fig. 33). Brown diamonds occur in all diamond deposits but are particularly common in the Argyle mine in Australia.

These vacancy clusters must form at temperatures where diamond is still capable of being deformed plastically (>900 °C, DeVries 1975), meaning that these defects are created at some point after diamond has crystallized in the mantle but before it is transported to the crust. Presumably some form of differential stress produced by mantle flow or the initial stages of incorporation and transport by the kimberlite magma may be responsible.
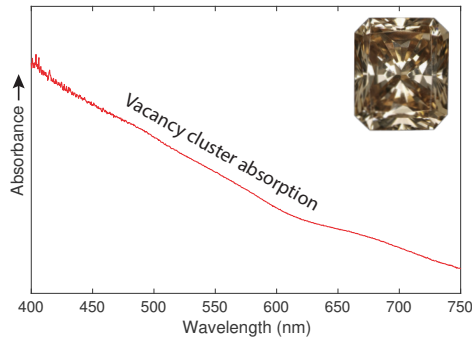
Figure 33. Brown color in most natural diamonds is a result of absorption by large vacancy clusters which are produced by plastic deformation. The absorption itself is characteristically broad and devoid of sharp optical transitions.

Pink to red diamonds

Some of the most valuable gem diamonds occur with pink to red hues that are also thought to be partially produced by plastic deformation of the diamond lattice. Red diamonds were among the first colored diamonds to approach US $1M per carat at auction (the Hancock Red; Christies 2020). Unlike their brown counterparts, pink and red diamonds are extremely rare and apparently represent a unique circumstance of plastic deformation that produces a broad absorption band centered around 550 nm (Fig. 34a). The 550 nm band occurs both in diamonds with and without nitrogen impurities (Type Ia and IIa), but the pink to red color distribution is quite different depending on the aggregation state of the impurities (Gaillou et al. 2010; Eaton-Magaña et al. 2018b, 2020). Pink Type IIa diamonds show even color distribution, while the pink color in Type Ia diamonds is concentrated in colored lamellae that indicate discrete zones of plastic deformation. These lamellae even take on a different appearance depending on the aggregation state and concentration of nitrogen in the diamonds. Dominantly Type IaA diamonds which mostly hail from Russia (the Lomonosov mine and others) show well developed pink lamellae separated by zones with no color at all (Howell et al. 2015; Eaton-Magaña et al. 2018b). Lower nitrogen, dominantly Type IaAB to IaB, pink to red diamonds from the Argyle mine in Australia tend to have much more closely spaced pink lamellae where the color blends between them (Eaton-Magaña et al. 2018b). Little is known about the atomic structure of the defect which produces the 550 nm absorption band, but it has been shown to be temporarily reduced in intensity by exposure to strong UV light, suggesting some charged analogue also exists to facilitate a charge transfer bleaching effect (Khan et al. 2009, 2010; Eaton-Magaña et al. 2018b, 2020). Recent work has linked the 550 nm absorption band to a broad photoluminescence band at ~660 nm (Gaillou et al. 2010; Eaton-Magaña et al. 2018b, 2020).
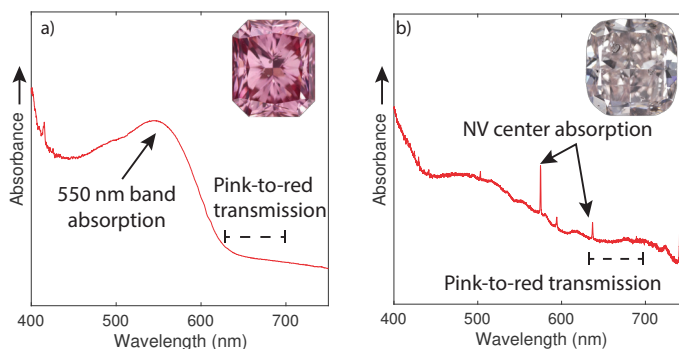
Figure 34. Natural pink to red diamonds are usually colored by a 550 nm absorption band caused by plastic deformation (**a**), but on extremely rare occasions can be colored by nitrogen-vacancy center absorption (**b**). In contrast, nitrogen-vacancy absorption and emission is extremely common in synthetic diamond grown by chemical vapor deposition. Spectra collected with samples at 80 K.

Pink to red color can also be generated in diamond by relatively high concentrations of nitrogen-vacancy (NV) centers (Fig. 34b). In natural diamonds, this occurrence is extremely rare and typically produces pale pink colors, many of which are thought to originate from the historically important Golconda region in India (Fritsch 1998) so that diamonds of this hue are known as Golconda pink regardless of origin. However, through irradiation and annealing treatment of diamonds containing C centers, high concentrations of NV can be created to produce a saturated pink to red color. Additionally, many synthetic diamonds also contain C centers and can be treated to produce pink to red color via absorption and emission at the NV defect.

Blue diamonds

Blue color in diamond is most commonly produced by the presence of uncompensated boron in the lattice, also making the stones semiconducting. Boron absorbs light strongly in the infrared region extending as a continuum into the visible range to produce a blue hue (Fig. 35). Boron absorbs so strongly that only a few hundred parts per billion are adequate to produce blue color in most diamonds (Eaton-Magaña et al. 2018a). Many famous blue gem diamonds like the Hope diamond owe their color to boron. In 2015, US \$4M/carat was paid for a 12.03 carat blue diamond known as the Blue Moon of Josephine (Associated Press 2015), then the highest per-carat price ever achieved for a diamond.
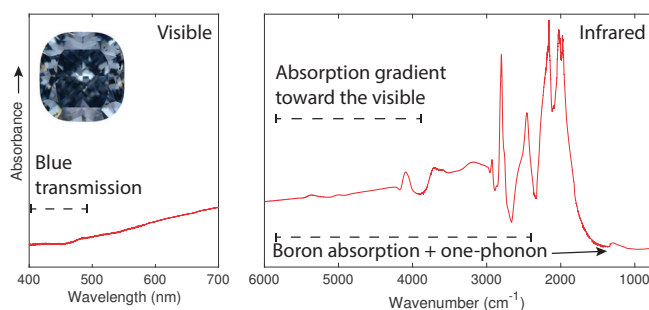
Figure 35. The most common cause of blue color in diamond is boron impurities that absorb strongly in the infrared region (**right**) with an absorption continuum that extends into the visible range (**left**) to produce the blue color.

Type IIb diamonds like these are among the rarest of gem diamonds. Recent work has shown that many Type IIb diamonds (as well as large, pure Type IIa stones) contain mineral inclusions originating from as deep as 660 km in the Earth (Smith et al. 2018). This model suggests boron introduction from seawater to an altered slab that subducted to those depths where the diamond was formed. While Type IIb diamonds occur in deposits around the world, a few mines, like the Cullinan mine (formerly Premier) in South Africa are known to produce higher numbers of these stones. Blue Type IIb diamonds can also be grown in a laboratory through introduction of boron into the growth chamber (for CVD growth) or growth capsule (for HPHT growth). Typically, the more boron added, the deeper the color saturation. At higher boron concentration, above a few ppm, the diamond starts appearing black.

Blue color can also be produced by relatively high amounts of radiation damage to the diamond lattice, either naturally or during irradiation treatment. Neutral vacancy defects (GR1) absorb very strongly in the red end of the visible spectrum, and when they occur in high enough concentrations, that absorption overwhelms any other absorptions due to nitrogen impurities and produces a blue hued diamond (Fig. 36a). In nature, blue color only occurs very rarely as a product of strong localized beta or gamma irradiation that penetrates to great depths in the diamond. A few such natural diamonds have been recovered in South America and central Africa (Draper 1951; Themelis 1987). Surficial alpha damage produces green color, as discussed below. Blue color can readily be added to natural or synthetic diamond using electron or gamma-ray irradiation to produce large quantities of vacancies.

Green diamonds

Most green diamonds derive their color from vacancy defects (GR1) that absorb light in the red region of the visible spectrum. These individual vacancies are created, along with interstitial defects, when diamonds are exposed to a source of radiation, either naturally in the Earth or in a laboratory. As discussed in previous sections, vacancies become mobile at relatively low temperatures (~700 °C) and can dominate the dynamics of defect and color center production (Collins 2001).

The appearance of radiation damage in diamond varies depending on the source of radiation. Alpha particles only penetrate to depths of 20–30 μm and usually produce green colored spots (called radiation stains by gemmologists) at or just below the diamond natural surface. These spots change almost instantly to a brown color at around 550 °C or possibly lower temperatures with prolonged residence in the Earth (Nasdala et al. 2013; Eaton-Magaña and Moe 2016). Beta radiation is more penetrative and causes internal zones of color. Gamma radiation usually affects the entire diamond. In nature, most radiation damage is thought to occur through prolonged interaction with fluids in shallow crustal environments, either in the kimberlite host or, more commonly, in an alluvial setting. However, the occurrence of radioactive mineral grains adjacent to diamond in its host rock cannot be ruled out as a source of damage in many cases. Regardless of the source, due to the relatively low thermal stability of vacancy defects in diamond, the radiation damage must occur at shallow levels in the Earth's crust. For natural diamonds, the uranium-thorium decay sequence is the most likely radiation source as it is the most abundant in the Earth. Laboratory electron irradiation (or occasionally gamma irradiation) treatments are commonly used to change the color of both natural and synthetic diamonds to create green diamonds.

Generally, as vacancy concentration increases, the saturation of green color also increases until the color of the diamond starts to take on a blue color component at higher amounts of radiation damage (Fig. 36a). The presence of other defects in combination with vacancies may significantly impact the diamond color. Most natural diamonds contain nitrogen impurities that absorb strongly in the blue region of the visible spectrum. The combination of nitrogen absorption with GR1 absorption usually results in a green to yellow-green diamond color (Fig. 36b). Another important consideration for green color in diamond is distribution of the radiation damage.
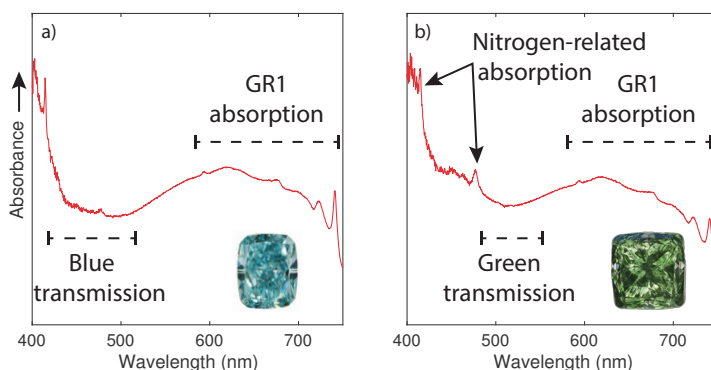
Figure 36. Isolated neutral vacancies, produced by radiation damage, produce an absorption known as GR1 (with its ZPL at 741 nm and a broad vibronic band which reaches approximately 575 nm) and can result in a blue color in diamond when their concentrations are very high and other defects are absent **(a)**. When nitrogen impurities are present, GR1 defects are the most common cause of green color **(b)**. Spectra collected with samples at 80 K.

Most natural diamonds only see significant surficial damage with very shallow color zones near radiation stains or thin "skins" of green color on the outer rim of the crystals produced by alpha irradiation (Vance and Milledge 1972; Vance et al. 1973; Breeding et al. 2018) Natural diamonds with green body color (internal color zones) are extremely rare and represent unique conditions in the Earth where significant beta or gamma exposure has occurred over geologic time. One of the most famous green diamonds is the Dresden Green, a 41-carat stone thought to originate from India (Hough 1913; Rosch 1957; Bosshart 1989, 1994). While green diamonds can occur in many deposits worldwide, they are most commonly found in South America, Zimbabwe, and the Central African Republic (Draper 1951; Themelis 1987; Breeding et al. 2018).

Violet diamonds

Amongst the rarest of gem diamonds are those that exhibit a deep violet color. The violet color is a result of a combination of defects including nitrogen defects such as N3 that absorb <450 nm, a broad band centered at ~530–540 nm that may be due to plastic deformation, and a broad absorption band centered at ~720 nm that is only observed in diamonds with high concentrations of hydrogen-related defects (van der Bogert et al. 2009; Eaton-Magaña et al. 2018a) (Fig. 37). These stones are only sourced from the Argyle mine in Australia, suggesting that they may very well be an analogue of the pink diamonds discovered there, but
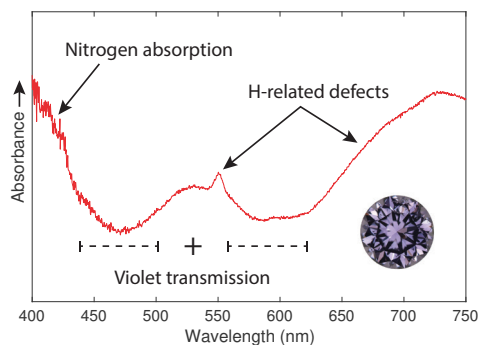
Figure 37. Violet color in diamond results from a combination of hydrogen-related absorptions, nitrogen absorptions and a broad band at 530–540 nm. Those absorptions labelled "H-related" have only been observed in high hydrogen-diamonds, but their origin is unknown (van der Bogert et al. 2009; Eaton-Magaña et al. 2018a). Spectrum collected with sample at 80 K.

with additional hydrogen impurities. Stones with similar hydrogen and nitrogen defects but missing the ~530 nm band tend to be grey to brown to green in color.

TREATMENTS TO CHANGE THE COLOR OF DIAMOND

Many Type IaA diamonds and some Type IIa diamonds have very little absorption in the visible region and so are colorless or near-colorless. Most diamonds, however, have some tint of color to them (either yellowish from nitrogen or brownish from plastic deformation), and the origins of these colors have been discussed in the preceding section. Occasionally some of these colors are very attractive, and diamonds which have a "fancy" color can be command a very high selling price. Many diamonds, however, have an insipid color (usually pale yellow, pale brown, or grey) which makes them less desirable than near-colorless or fancy-colored diamonds of the same size. In certain cases, the color of a diamond can be improved by some form of treatment. In this section we briefly consider various methods by which the color of a diamond can be changed. The defects involved have been considered in the preceding two sections.

In the gemological world, treatment is considered anything other than cutting and polishing that is done to a gemstone to change its natural appearance and thus improve its desirability. In the case of diamond, treatments generally cause enhancements to either the color or clarity of the stone and may include coatings, laser drilling, filling of fractures with glass, or rearrangement of atoms in the lattice. Our discussion will focus on ways in which the atomic structure of diamond is re-engineered to produce a particular color or attempt to remove color completely. The primary lattice-based treatments commonly applied to diamond are irradiation (with or without subsequent annealing), high pressure, high temperature annealing (usually performed at ~5–6 GPa and ~1800–2100 °C), or a combination thereof.
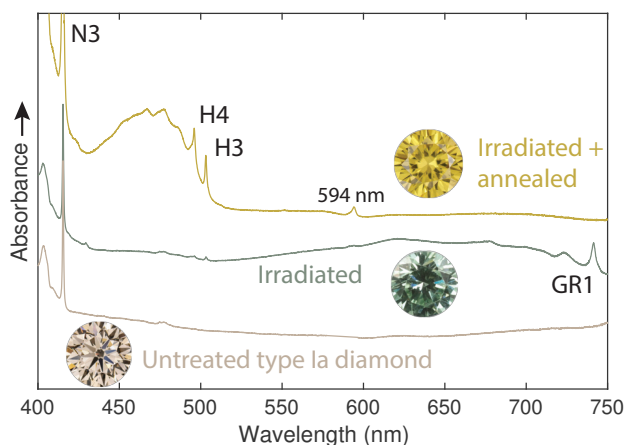
Irradiation

Irradiation of Type Ia or Type IIa diamond with high-energy electrons creates vacancies and interstitials, leading to a blue, blue-green, or green color, depending on the energy of the electrons used for the irradiation and absorptions from pre-existing nitrogen-related defects (Fig. 38). Irradiation with neutrons produces vacancies and interstitials, as well as more extensive radiation-damage products which absorb more strongly in the blue region of the visible spectrum. Neutron-irradiated diamonds therefore have a green color, and at high doses will simply appear black. Most commercial diamond treaters perform a "stabilization" annealing at ~500 °C following any irradiation treatment to remove many of the numerous low-binding-energy defects which are created by irradiation, in addition to the small population of close-proximity and highly strained vacancy-interstitial defects (Iakoubovskii et al. 2003). These defects have a minor effect on the color overall, but when removed, the color of the diamond shifts slightly to a more stable hue, suggesting that the interstitial defects may undergo some minor photo- or thermo-chromism, presumably due to changes in charge state.

When an irradiated Type Ia diamond is annealed at approximately 800 °C, the vacancies become mobile and wander through the diamond until they are trapped at one of the forms of nitrogen. A vacancy trapped at an A center produces an H3 center (N_2V^0), and a vacancy trapped at a B center results in an H4 center ($N_4V_2^0$; Fig. 38). The absorption bands associated with these centers occur at the blue end of the visible region and the diamonds consequently have a yellow color—similar to that of some fancy yellow diamonds in which the color is due to single nitrogen (Figs. 11a, 32b) or the N2 and N3 systems (Figs. 7, 32a).

The heating of an electron-irradiated Type Ia diamond to approximately 1400 °C, may generate absorption by the H2 (N_2V^-) center as a result of the production of H3 (N_2V^0) and subsequent charge transfer between H3 and isolated substitutional nitrogen (C centers). In favorable cases this treatment can give the diamond an attractive green color (Collins 2001).

Figure 38. Irradiation treatment of a Type Ia diamond creates GR1 (V0) defects that produce green color. Annealing of the diamond at 800 °C produces H3 and H4 defects due to migration and combination of vacancy defects with A and B centers and creates yellow color. Spectra collected with samples at 80 K.

Irradiation of Type Ib diamond generates vacancies principally in the negative charge state (because of the large concentration of nitrogen donors). The absorption associated with V^- is referred to spectroscopically as the ND1 center, and is in the UV region with a ZPL at 394 nm. The absorption by the isolated substitutional nitrogen, in combination with weak GR1 absorption produced by the irradiation, gives the diamond an unattractive drab green color (Fig. 39). After annealing at 800 °C, vacancies become trapped at the single-nitrogen centers
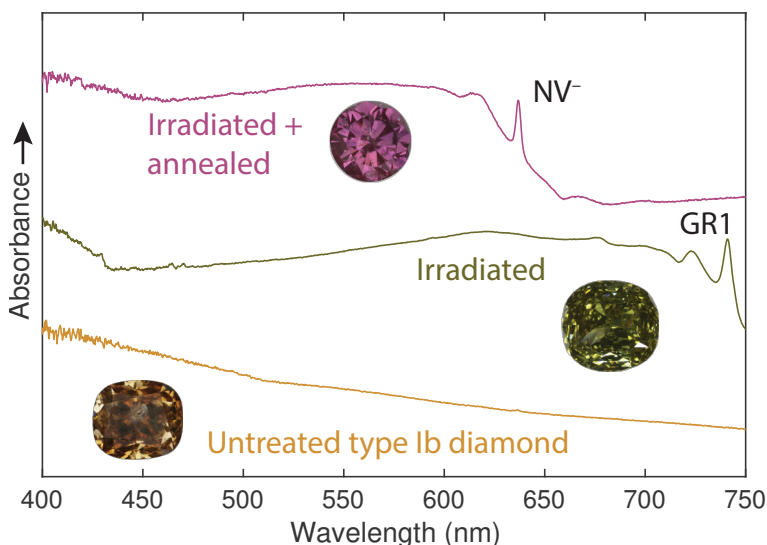
Figure 39. Irradiation treatment of a brown Type Ib diamond creates V^- (not shown) as well as the V^0 that produces a dull green color. Annealing of the diamond at 800 °C generates a combination of vacancy-related defects (largely negatively charged due to C centers being donors) and creates pink to red color. Spectra collected with samples at 80 K.

to produce the negative nitrogen-vacancy center NV⁻. The absorption produced by this center gives the diamond a pink to red color which, to the eye, is similar to that of natural pink diamonds described in the previous section.

HPHT treatment

Many natural diamonds have a brown color produced by the presence of vacancy clusters (see *Brown diamonds*). These vacancy clusters can be partially dissociated by annealing under HPHT conditions. In Type IIa diamond the released vacancies are trapped at dislocations or diffuse to the surface, and the net effect is to reduce the brown color. Occasionally HPHT treatment of Type IIa diamonds yields samples with a slight pink hue if a 550 nm absorption band originally coexisted with the vacancy clusters causing the brown color, or blue color if compensated boron is freed by the treatment to become uncompensated (Hall and Moses 2000).

When Type Ia diamonds are HPHT treated, the vacancies become trapped at A centers, producing H3 centers. The net effect is to reduce the brown component and increase the yellow component of the color, resulting in an overall improvement in appearance. H3 centers also produce green luminescence to visible light which sometimes appears as a greenish tint on the yellow body color. The results described are achieved with annealing temperatures around $1800\,°C$. If the treatment temperature is increased to 2000 to 2100 °C then, in addition, some of the A nitrogen dissociates to form single nitrogen atoms. As with low-temperature annealing described above, charge transfer between H3 and substitutional nitrogen (N_2V^0 and N_s^0, yielding N_2V^- and N_s^+) can add a green component to the color due to the H2 (N_2V^-) absorption.

Natural Type Ia diamonds containing a modest concentration of N3 centers may have a "tinted" yellow color which is neither near-colorless nor fancy yellow. HPHT annealing at sufficiently high temperatures to dissociate some of the A nitrogen produces absorption at the blue end of the visible spectrum (Figs. 11a, 32b), due to the production of single nitrogen, thereby enhancing the yellow color or adding a significant orange color component if enough single nitrogen atoms are created.

Combination treatments

Starting with an off-color Type Ia diamond it is also possible to produce a pink diamond by a three-stage process: HPHT annealing to produce single nitrogen; irradiation to produce vacancies: annealing at 800 °C to produce NV⁻ centers. Similarly, a two-stage process is now commonly used to create vivid blue color. The off-color diamond is HPHT annealed to remove brown color (but not at high enough temperature to create isolated nitrogen) and subsequently irradiated with high energy electrons to impart the saturated blue hue. This treatment allows for a much more attractive product than simply irradiating an off-color diamond.

In the last decade, treaters have also begun to employ a very low dose electron irradiation treatment and sometimes low temperature annealing following HPHT processing of Type II diamonds. This is an attempt to add back certain defects that are known to be removed by HPHT and are used for identification of natural and treated diamonds by gem laboratories. These post-HPHT treatments have no effect on the color of the diamond and are performed with the sole purpose of attempting to fraudulently pass treated diamonds as naturally colored stones (Eaton-Magana and Breeding 2016).

Although the colors produced by various treatments are similar to colors that occur naturally, examination of the diamonds using optical spectroscopy allows most naturally colored and treated diamonds to be differentiated.

## USING OPTICAL SPECTROSCOPY TO DETECT TREATED DIAMOND

Proper disclosure of gemstone treatments is explicitly required by law in nearly every country, but many treated diamonds are bought, sold, or submitted to gem laboratories undisclosed every day. Treated-color gem diamonds are worth anywhere from 50% less to several orders of magnitude less than their natural color equivalents, simply due to the rarity of the finest natural color stones. This huge discrepancy in pricing generally requires that colored diamonds be sent to gemological laboratories for certification before sale. While traditional gemological tools like the microscope, handheld spectroscope, and fluorescence lamp are still useful for some identification needs, modern atomic lattice-based treatments of diamond require the use of spectroscopic analytical instruments for proper detection (Overton and Shigley 2008; Breeding et al. 2010). The value of diamond dictates that analysis be done in a non-destructive manner, making optical spectroscopy the primary tool used for identification. Specifically, infrared (IR) and ultraviolet–visible (UV–Vis) absorption spectroscopy and photoluminescence (PL) spectroscopy are the most commonly employed methods of detecting treatments in gem diamond, and are employed even in the analysis of low-value gemstones such as melee. Certain analytical techniques have proven more effective for identification of each of the major diamond color treatments discussed in the previous section—HPHT treatment and irradiation treatment—and combinations of these treatments usually show some characteristics of both.

Detection of HPHT treatment

As mentioned in the preceding section, HPHT treatment has drastically different goals and results depending on the diamond type of the sample being treated. In general, most treated Type II diamonds have undergone HPHT treatment to remove brown color and produce a near colorless stone, or in some cases a pink or blue diamond color (Hall and Moses 2000; Fisher 2009). Most natural diamonds are Type Ia, with approximately 1.3% being Type II (Smith et al. 2016) and having the potential to be decolorized. For near colorless diamonds, then, the basic screening method is to evaluate diamond type using IR spectroscopy to separate Type II samples. With only a few rare exceptions, Type Ia near colorless diamonds can safely be concluded to be natural color. Among those stones determined to be Type II, PL spectroscopy is employed to search for defects either added or removed by the treatment process (Fisher and Spits 2000; Eaton-Magaña and Breeding 2016). Fortunately, in order to dramatically increase the speed at which the atoms rearrange (depending exponentially on temperature), temperatures employed during HPHT treatment are significantly higher than those experienced by most natural diamonds of approximately 1050–1200 °C (Stachel and Harris 2008; Stachel and Luth 2015). Several natural centers are unstable at HPHT conditions and are annealed from the stone or reconfigured into other defects. Other defects change their charge state due to the production of new electron donors by dissociation of minute amounts of aggregated nitrogen (A centers primarily) to form C centers (Brozel et al. 1978). Despite being classified as Type IIa, most near-colorless diamonds of this type contain some nitrogen impurities in the form of NV or H3 defects that can be detected down to several parts-per-billion by PL spectroscopy.

The creation of C center donors during HPHT treatment causes some of the NV centers to convert from the neutral state (NV^0) to the negative charge state (NV^-) and H3 centers (N_2V^0) to convert to their negatively charged equivalents, H2 centers (N_2V^-) (Chalain et al. 2000; Collins et al. 2000; Fisher and Spits 2000; Lim et al. 2010) (Fig. 40). Thus, a detected ZPL height ratio of NV^-/NV^0 >1 (at 80 K using 514 nm laser excitation: the laser wavelength will affect this ratio) and significant H2 emission in near-colorless diamonds strongly suggests that HPHT treatment has occurred.

For brownish Type Ia diamonds, HPHT treatment at approximately 1800 °C typically adds color by creation of more color centers like H3 and C centers. As vacancy clusters are
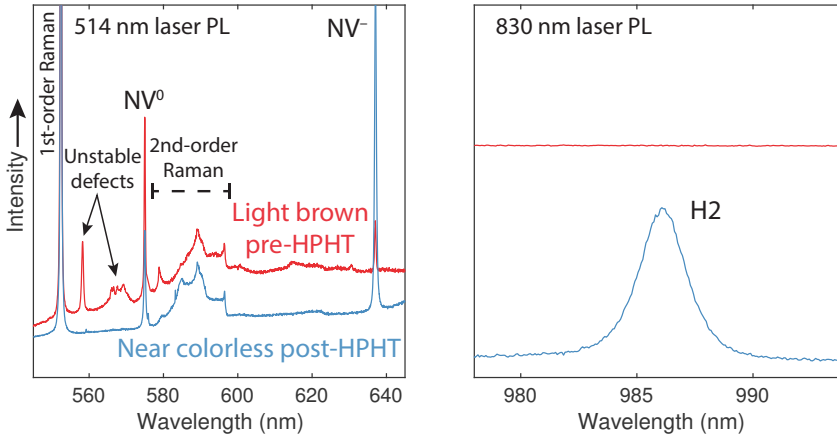
Figure 40. Photoluminescence spectroscopy reveals that unstable defects are removed by HPHT treatment of Type IIa brown diamonds to decolorize them. In addition, the NV^-/NV^0 ratio increases to >1 in treated diamonds (as measured with PL using a 514 nm laser). The H2 defect is rare in untreated natural samples and can be used in combination with other spectroscopic markers to identify treated diamonds. Spectra collected with the samples at 80 K.

destroyed by HPHT treatment (Mäki et al. 2009), the individual vacancies migrate through the lattice and become trapped at abundant A centers to generate H3 defects that produce yellow color (and sometimes a green luminescence overtone as well) (Collins et al. 2000). H4 centers—produced at lower temperatures (around 800 °C) when vacancies are trapped at B centers—are not stable at HPHT conditions. H4 centers do not form during HPHT treatment even in diamonds containing high concentrations of B centers. At higher treatment temperatures (>2000 °C), aggregated nitrogen dissociates to create significant numbers of C centers which also add yellow color (Collins et al. 2000). Absorption (UV–Vis and IR) spectroscopies are more useful for identification in these cases. Liquid nitrogen temperature UV–Vis shows that H3, C centers, and sometimes H2 are responsible for the color, a relatively uncommon occurrence for natural yellow or green color as discussed in *Green diamonds*. Infrared spectroscopy often shows the occurrence of C centers (1344 cm^{-1}) along with both A and B centers, another condition that is extremely rare in untreated natural diamonds (Fig. 41). In addition, platelets are usually significantly reduced by the treatment, a feature that can easily be recognized in IR spectroscopy in combination with the occurrence of C centers (Reinitz et al. 2000) (Fig. 41).

Detection of irradiation treatment (including subsequent annealing)

Unlike HPHT treatment where the temperatures are higher than natural diamond settings, irradiation treatment involves nearly identical conditions and results to those that occur naturally in the Earth (Fig. 42). The only major difference is the timescale—a few minutes in a lab compared to hundreds to millions to billions of years in the Earth—but, unfortunately, few measurable spectroscopic characteristics seem to be tied to the timescale. Consequently, whether irradiation occurred in the Earth or a laboratory is sometimes difficult to determine, leading to a higher percentage of "undetermined" color origin assessments on laboratory reports of green diamonds.

Photoluminescence spectroscopy has proven useful in detecting, in treated diamonds, some interstitial-related defects that are typically annealed out naturally by long residence times at elevated temperatures experienced by natural color diamonds in the Earth (Breeding et al. 2018). Observations of natural radiation damage on the surface of these stones provides
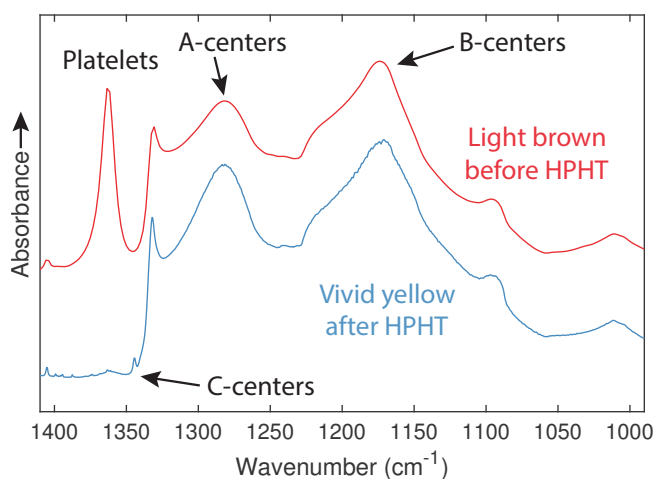
Figure 41. HPHT treatment of Type Ia diamonds usually causes a noticeable decrease in platelet concentration and, if the treatment temperature is >2000 °C, the presence of C centers can usually be detected along with A and B centers. Baseline offset for clarity.
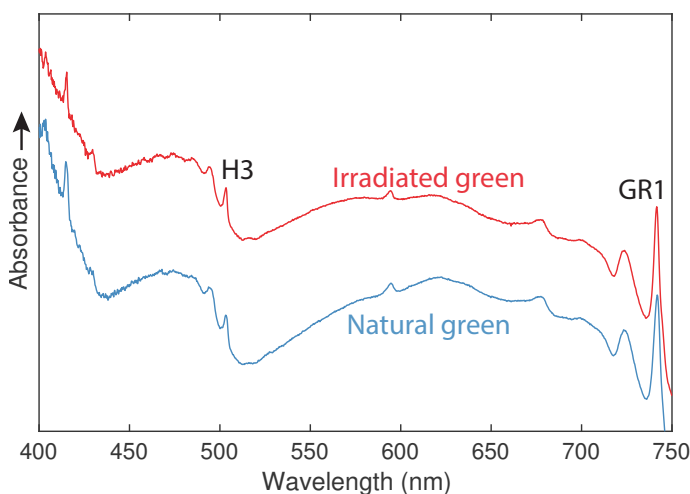
Figure 42. Natural irradiaton in the Earth and laboratory irradiation using electrons often results in very similar defect structures and green colors in gem diamond, making the separation difficult in some cases, especially if the pre-treatment material is natural (as is the case here). Spectra collected with the samples at 80 K.

some evidence that a natural radiation source was present at some time in the diamond's history. More useful, however is the post-irradiation annealing treatment process that is often done at different temperatures to produce yellow, pink to red, or orange diamonds. Heating irradiated Type Ia diamonds at 800 to 1400 °C causes vacancies to become trapped at nitrogen impurities to create H3, H4, or NV defects that give rise to the newly treated diamond colors. A by-product of engineering these color centers is the creation of several other defects that do not typically occur with high absorption intensity in equivalent natural color stones, including the 594 nm center, H1a (1450 cm^{-1}), H1b (4935 cm^{-1}), and H1c (5165 cm^{-1}) (Zaitsev 2001;

Collins 2003, Fig. 43). The 594 nm absorption center can be detected by UV–Vis absorption spectroscopy (at liquid nitrogen temperature), while the others absorb distinctly in IR spectra (Fig. 43). These centers are believed to be nitrogen-containing interstitial centers which have been shown to anneal out between 1100 and 1400 °C (Collins et al. 2005; Liggins et al. 2010). Therefore, the presence of these absorption peaks with significant intensity in Type Ia diamonds strongly suggests the possibility of irradiation and annealing treatments.
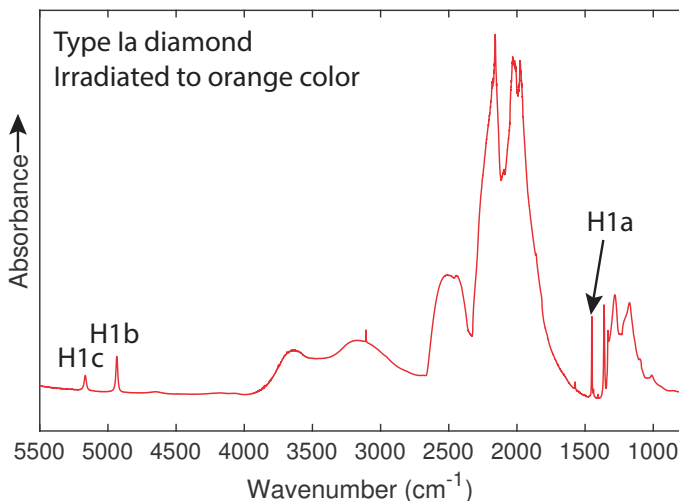
Figure 43. After irradiation and annealing treatments, Type Ia diamonds often develop H1a, H1b, and H1c defects in significant concentrations. These defects are extremely rare in natural color diamonds.

SUMMARY

Diamond is an extreme material with a rich history at the forefront of physical and spectroscopic understanding, driven by its economic value in both cosmetic and technological applications. The relatively recent ability to synthesise high-quality diamond with superb control over impurities and growth morphology has been instrumental in the development of our understanding of defect and impurity processes within natural diamond. Combined with recent spectroscopic advances such as the ability to optically interrogate and monitor a single atomic defect, diamond continues to drive spectroscopy theory and practice. The authors are confident that these updated techniques will continue to shed further light on diamond growth and evolution, and ultimately the geological processes which drive them in nature.

ACKNOWLEDGEMENTS

REFERENCES

Achard J, Silva F, Brinza O, Tallaire A, Gicquel A (2007) Coupled effect of nitrogen addition and surface temperature on the morphoFy and the kinetics of thick CVD diamond single crystals. Diamond Relat Mater 16:685–689

Achard J, Jacques V, Tallaire A (2020) Chemical vapour deposition diamond single crystals with nitrogen-vacancy centres: A review of material synthesis and technology for quantum sensing applications. J Phys D: Appl Phys 53:313001

Aharonovich I, Neu E (2014) Diamond nanophotonics. Adv Opt Mater 2:911–928

Allen BP, Evans T (1981) Aggregation of nitrogen in diamond, including platelet formation. Proc R Soc London, Ser A 375:93–104

Allers L, Collins AT, Hiscock J (1998) The annealing of interstitial-related optical centres in Type II natural and CVD diamond. Diamond Relat Mater 7:228–232

Ashfold MNR, Goss JP, Green BL, May PW, Newton ME, Peaker CV (2020) Nitrogen in Diamond. Chem Rev 120:5745–5794

Aslam N, Waldherr G, Neumann P, Jelezko F, Wrachtrup J (2013) Photo-induced ionization dynamics of the nitrogen vacancy defect in diamond investigated by single-shot charge state detection. New J Phys 15:013064

Associated Press (2015) Rare blue diamond sells for record $48.5 million at auction. NBC News, www.nbcnews.com/business/markets/rare-blue-diamond

Atatüre M, Englund D, Vamivakas N, Lee S-Y, Wrachtrup J (2018) Material platforms for spin-based photonic quantum technologies. Nat Rev Mater 3:38–51

Awschalom DD, Hanson R, Wrachtrup J, Zhou BB (2018) Quantum technologies with optically interfaced solid-state spins. Nat Photonics 12:516–527

Baker JM, Newton ME (1994) The use of ENDOR to identify the atomic structure of defects in diamond. Appl Magn Reson 7:209–235

Barry JF, Schloss JM, Bauch E, Turner MJ, Hart CA, Pham LM, Walsworth RL (2020) Sensitivity optimization for NV-diamond magnetometry. Rev Mod Phys 92:015004

Bassett LC, Alkauskas A, Exarhos AL, Fu KC (2019) Quantum defects by design. Nanophotonics

Bosshart G (1989) The Dresden Green. J Gemmol 21:351

Bosshart G (1994) Investigations mordernes du diamant vert de Dresden et interpretation des resultats. Revue de Gemmologie 121:5

Breeding CM, Shen AH, Eaton-Magaña S, Rossman GR, Shigley JE, Gilbertson AM (2010) Developments in gemstone analysis techniques and instrumentation during the 2000s. Gems Gemol 46:241–257

Breeding CM, Eaton-Magaña S, Shigley JE (2018) Natural-color green diamonds: a beautiful conundrum. Gems Gemol 54:2–27

Breeze BG, Meara CJ, Wu XX, Michaels CP, Gupta R, Diggle PL, Dale MW, Cann BL, Ardon T, D'Haenens-Johansson UFS, Friel I (2020) Doubly charged silicon vacancy center, Si-N complexes, and photochromism in N and Si codoped diamond. Phys Rev B 101:184115

Breuer SJ, Briddon PR (1996) Energy barrier to reorientation of the substitutional nitrogen in diamond. Phys Rev B 53:7819

Brozel MR, Evans T, Stephenson RF (1978) Partial dissociation of nitrogen aggregates in diamond by high temperature-high pressure treatments. Proc R Soc London, Ser A 361:109–127

Bruley J, Brown LM (1989) Quantitative electron energy-loss spectroscopy microanalysis of platelet and voidite defects in natural diamond. Philos Mag A 59:247–261

Bulanova GP (1995) The formation of diamond. J Geochem Explor 53:1–23

Callister WD (2006) Materials Science and Engineering: An Introduction, 7th ed. Wiley, Hoboken

Cann BL (2009) Thesis: Magnetic resonance studies of point defects in diamond. University of Warwick

Chakravarthi S, Moore C, Opsvig A, Pederson C, Hunt E, Ivanov A, Christen I, Dunham S, Fu KMC (2020) Window into NV center kinetics via repeated annealing and spatial tracking of thousands of individual NV centers. Phys Rev Materials 4:023402

Chalain J-P, Fritsch E, Hänni HA (2000) Identification of GE POL diamonds: A second step. J Gemmol 27:73–78

Chen Y-C, Griffiths B, Weng L, Nicley S, Ishmael SN, Lekhai Y, Johnson S, Stephen CJ, Green BL, Morley GW, Newton ME (2019) Laser writing of individual atomic defects in a crystal with near-unity yield. Optica 6:662–666

Chevallier J, Theys B, Lusson A, Grattepain C, Deneuville A, Gheeraert E (1998) Hydrogen-boron interactions in p-type diamond. Phys Rev B 58:7966–7969

Chrenko RM, Tuft RE, Strong HM (1977) Transformation of the state of nitrogen in diamond. Nature 270:141–144

Christies (2020). https://www.christies.com/features/10-jewels-that-created-auction-history-and-changed-the-market-9549-3.aspx. Retrieved on 2021/02/05

Clark CD, Ditchburn RW, Dyer HB (1956a) The absorption spectra of irradiated diamonds after heat treatment. Proc R Soc London, Ser A 237:75–89

Clark CD, Ditchburn RW, Dyer HB (1956b) The absorption spectra of natural and irradiated diamonds. Proc R Soc London, Ser A 234:363–381

Collins AT (1977) Radiation damage in natural semiconducting diamond. In NB Urli and JW Corbett, Eds., Radiation Effects in Semiconductors 1976 (Institute of Physics Conference Series 31), p 346–353

Collins AT (1980) Vacancy enhanced aggregation of nitrogen in diamond. J Phys C: Solid State Phys 13:2641–2650

Collins AT (2001) The colour of diamond and how it may be changed. J Gemmol 27:341–359

Collins AT (2002) The Fermi level in diamond. J Phys: Condens Matter 14:3743–3750

Collins AT (2003) The detection of colour-enhanced and synthetic gem diamonds by optical spectroscopy. Diamond Relat Mater 12:1976–1983

Collins AT, Kiflawi I (2009) The annealing of radiation damage in Type Ia diamond. J Phys: Condens Matter 21:364209

Collins AT, Mohammed K (1982) Optical studies of vibronic bands in yellow luminescing natural diamonds. J Phys C: Solid State Phys 15:147–158

Collins AT, Williams AWS (1971) The nature of the acceptor centre in semiconducting diamond. J Phys C: Solid State Phys 4:1789–1800

Collins AT, Woods GS (1982) Cathodoluminescence from "giant" platelets, and of the 2.526 eV vibronic system, in Type Ia diamonds. Philos Mag Part B 45:385–397

Collins AT, Lightowlers EC, Dean PJ (1969) Role of phonons in the oscillatory photoconductivity spectrum of semiconducting diamond. Phys Rev 183:725

Collins AT, Kanda H, Burns RC (1990) The segregation of nickel-related optical centres in the octahedral growth sectors of synthetic diamond. Philos Mag B: 61:797–810

Collins AT, Kanda H, Kitawaki H (2000) Colour changes produced in natural brown diamonds by high-pressure, high-temperature treatment. Diamond Relat Mater 9:113–122

Collins AT, Connor A, Ly C-H, Shareef A, Spear PM (2005) High-temperature annealing of optical centers in Type-I diamond. J Appl Phys 97:083510–083517

Cox A, Newton ME, Baker JM (1994) 13 C, 14 N, 15 N ENDOR measurements on the single substitutional nitrogen centre (P1) in diamond. J Phys: Condens Matter 6:551–563

Coxon DJL, Staniforth M, Breeze BG, Greenough SE, Goss JP, Monti M, Lloyd-Hughes J, Stavros VG, Newton ME (2020) An ultrafast shakedown reveals the energy landscape, relaxation dynamics, and concentration of the N_3VH^0 defect in diamond. J Phys Chem Lett 11:6677–6683

Crisci A, Baillet F, Mermoux M, Bogdan G, Nesladek M, Haenen K (2011) Residual strain around grown-in defects in CVD diamond single crystals: A 2D and 3D Raman imaging study. Physica status solidi A 208:2038–2044

Crossfield MD, Davies G, Collins AT, Lightowlers EC (1974) The role of defect interactions in reducing the decay time of H3 luminescence in diamond. J Phys C: Solid State Phys 7:1909–1917

Cruddace RJ (2007) Thesis: Magnetic resonance and optical studies of point defects in single crystal CVD diamond. University of Warwick

D'Haenens-Johansson UFS, Edmonds AM, Green BL, Newton ME, Davies G, Martineau PM, Khan RUA, Twitchen DJ (2011) Optical properties of the neutral silicon split-vacancy center in diamond. Phys Rev B 84:245208

D'Haenens-Johansson UFS, Katrusha AN, Moe KS, Johnson P, Wang W (2015) Large colorless HPHT-grown synthetic gem diamonds from new diamond technology, Russia. Gems Gemol 51:260–279

D'Haenens-Johansson UFS, Butler JE, Katrusha AN (2022) Synthesis of diamonds and their identification. Rev Mineral Geochem 88:689–754

Dale MW (2015) Colour Centres on Demand in Diamond. Thesis, University of Warwick

Davies G (1976) The A nitrogen aggregate in diamond-its symmetry and possible structure. J Phys C: Solid State Phys, 9, L537–L542

Davies G (1979) Cathodoluminescence. *In:* The properties of diamond. JE Field (Ed.) Academic Press, London, p. 165–181

Davies G (1981) The Jahn–Teller effect and vibronic coupling at deep levels in diamond. Rep Prog Phys 44:787–830

Davies G (1999) Current problems in diamond: towards a quantitative understanding. Physica B 273–274:15–23

Davies G, Crossfield M (1973) Luminescence quenching and zero-phonon line broadening associated with defect interactions in diamond. J Phys C: Solid State Phys 6:L104–L108

Davies G, Welbourn CM, Loubser JHN (1978) Optical and electron paramagnetic effects in yellow Type Ia diamonds. Diamond Research, p. 23–30

Davies G, Lawson SC, Collins AT, Mainwood A, Sharp SJ (1992) Vacancy-related centers in diamond. Phys Rev B, 46:13157–13170

Dean PJ (1965) Bound excitons and donor-acceptor pairs in natural and synthetic diamond. Phys Rev 139:A588–A602

DeVries RC (1975) Plastic deformation and "work-hardening" of diamond. Mater Res Bull 10:1193–1199

Diggle PL, D'Haenens-Johansson UFS, Green BL, Welbourn CM, Tran Thi TN, Katrusha A, Wang W, Newton ME (2020) Decoration of growth sector boundaries with nitrogen vacancy centers in as-grown single crystal high-pressure high-temperature synthetic diamond. Phys Rev Materials 4:093402

Dischler B (2012) Handbook of Spectral Lines in Diamond. Springer-Verlag, Berlin

Doherty MW, Manson NB, Delaney P, Jelezko F, Wrachtrup J, Hollenberg LCLL (2013) The nitrogen-vacancy colour centre in diamond. Phys Rep 528:1–45

Draper T (1951) The diamond mines of Diamantina—Past and present. Gems Gemol 7:49–57

Dyer HB, Raal FA, Du Preez L, Loubser JHN (1965) Optical absorption features associated with paramagnetic nitrogen in diamond. Philos Mag 11:763–774

Eaton-Magaña S, Ardon T (2016) Temperature effects on luminescence centers in natural Type IIb diamonds. Diamond Relat Mater 69:86–95

Eaton-Magaña S, Breeding CM (2016) An introduction to photoluminescence spectroscopy for diamond and its applications in gemology. Gems Gemol 52:2–17

Eaton-Magaña S, Lu R (2011) Phosphorescence in Type IIb diamonds. Diamond Relat Mater 20:983–989

Eaton-Magaña SC, Moe KS (2016) Temperature effects on radiation stains in natural diamonds. Diamond Relat Mater 64:130–142

Eaton-Magaña S, Shigley JE, Breeding CM (2017) Observations on HPHT-grown synthetic diamonds: A review. Gems Gemol 53:262–285

Eaton-Magaña S, Breeding CM, Shigley JE (2018a) Natural-color blue, gray, and violet diamonds: Allure of the deep. Gems Gemol 54:112–131

Eaton-Magaña S, Ardon T, Smit KV, Breeding CM, Shigley JE (2018b) Natural-color pink, purple, red, and brown diamonds: Band of many colors. Gems Gemol 54:352–377

Eaton-Magaña S, McElhenny G, Breeding CM, Ardon T (2020) Comparison of gemological and spectroscopic features in Type IIa and Ia natural pink diamonds. Diamond Relat Mater 105:107784

Ekimov EA, Kondrin MV (2017) Vacancy–impurity centers in diamond: prospects for synthesis and applications. Physics-Uspekhi 60:539–558

Ekimov EA, Sidorov VA, Bauer ED, Mel'nik NN, Curro NJ, Thompson JD, Stishov SM (2004) Superconductivity in diamond. Nature 428:542–5

Etmimi K, Ahmed ME, Briddon PR, Goss JP, Gsiea AM (2009) Nitrogen-pair paramagnetic defects in diamond: A density functional study. Phys Rev B 79:205207

Evans T, Qi Z (1982) The kinetics of the aggregation of nitrogen atoms in diamond. Proc R Soc London, Ser A 381:159–178

Evans T, Kiflawi I, Luyten W, Tendeloo G Van, Woods GS (1995) Conversion of platelets into dislocation loops and voidite formation in Type IaB diamonds. Proc R Soc London, Ser A 449:295–313

Farrer RG (1969) On the substitutional nitrogen donor in diamond. Solid State Commun 7:685–688

Fedyanin DY, Agio M (2016) Ultrabright single-photon source on diamond with electrical pumping at room and high temperatures. New J Phys 18:073012

Felton S, Edmonds AM, Newton ME, Martineau PM, Fisher D, Twitchen DJ (2008) Electron paramagnetic resonance studies of the neutral nitrogen vacancy in diamond. Phys Rev B 77:081201

Fisher D (2009) Brown diamonds and high pressure high temperature treatment. Lithos 112:619–624

Fisher D, Lawson SC (1998) The effect of nickel and cobalt on the aggregation of nitrogen in diamond. Diamond Relat Mater 7:299–304

Fisher D, Spits RA (2000) Spectroscopic Evidence of GE POL HPHT-Treated Natural Type IIa Diamonds. Gems Gemol 36:42–49

Freitas JA, Klein PB, Collins AT (1994) Evidence of donor-acceptor pair recombination from a new emission band in semiconducting diamond. Appl Phys Lett 64:2136–2138

Fritsch E (1998) The nature of color in diamonds. *In:* The Nature of Diamonds. GE Harlow (ed) Cambridge University Press, p. 23–47

Fritsch E, Hainschwang T, Massi L, Rondeau B (2007) Hydrogen-related optical centres in natural diamond: An update. New Diamond Front Carbon Technol 17:63–89

Fujita N, Jones R, Öberg S, Briddon PR (2009) Large spherical vacancy clusters in diamond—Origin of the brown colouration? Diamond Relat Mater 18:843–845

Gaillou E, Post J., Bassim ND, Zaitsev AM, Rose T, Fries MD, Stroud RM, Steele A, Butler JE (2010) Spectroscopic and microscopic characterizations of color lamellae in natural pink diamonds. Diamond Relat Mater 19:1207–1220

Gali A, Lowther JE, Deák P (2001) Defect states of substitutional oxygen in diamond. J Phys: Condens Matter 13:11607–11613

Glover C, Newton M, Martineau P, Twitchen D, Baker J (2003) Hydrogen incorporation in diamond: The nitrogen-vacancy–hydrogen complex. Phys Rev Letters 90:185507

Goss JP, Briddon PR (2006) Theory of boron aggregates in diamond: First-principles calculations. Phys Rev B 73:085204

Goss JP, Coomer BJ, Jones R, Fall CJ, Briddon PR, Öberg S (2003) Extended defects in diamond: The interstitial platelet. Phys Rev B 67:165208

Goss JP, Briddon PR, Hill V, Jones R, Rayson MJ (2014) Identification of the structure of the 3107 cm^{-1} H-related defect in diamond. J Physics: Condens Matter 26:145801

Green BL (2013) Optical and Magnetic Resonance Studies of Point Defects in Single Crystal Diamond. Thesis, University of Warwick

Grimsditch MH, Anastassakis E, Cardona M (1978) Effect of uniaxial stress on the zone-center optical phonon of diamond. Phys Rev B 18:901–904

Hainschwang T, Simic D, Fritsch E, Deljanin B, Woodring S, DelRe N (2005) A gemological study of a collection of chameleon diamonds. Gems Gemol 41:20–35

Hainschwang T, Fritsch E, Notari F, Rondeau B (2012) A new defect center in Type Ib diamond inducing one phonon infrared absorption: The y center. Diamond Relat Mater 21:120–126

Hall M, Moses TM (2000) Gem Trade Lab Notes: Diamond—blue and pink HPHT annealed. Gems Gemol 36:254–255

Harris JW, Smit KV, Fedortchouk Y, Moore M (2022) Morphology of monocrystalline diamond and its inclusions. Rev Mineral Geochem 88:119–166

Hartland CB (2014) Thesis: A Study of Point Defects in CVD Diamond Using Electron Paramagnetic Resonance and Optical Spectroscopy. University of Warwick

Henry D (2020) Optical cathodoluminescence (Optical-CL). Retrieved 2021/01/20 from https://serc.carleton.edu/research_education/geochemsheets/opticalcl.html

Hirsch PB, Pirouz P, Barry JC (1986) Platelets, dislocation loops and voidites in diamond. Proc R Soc London, SerA 407:239–258

Hough E (1913) The great green diamond. Metropolitan Mag 38:9

Howell DW, Wood IG, Nestola F, Nimis P, Nasdala L (2012) Inclusions under remnant pressure in diamond: a multi-technique approach. Eur J Mineral 24:563–573

Howell DW, Fisher D, Piazolo S, Griffin WL, Sibley SJ (2015) Pink color in type I diamonds: Is deformation twinning the cause? Am Mineral 100:1518–1527

Howell DW, Collins AT, Loudin LC, Diggle PL, D'Haenens-Johansson UFS, Smit KV, Katrusha AN, Butler JE, Nestola F (2019) Automated FTIR mapping of boron distribution in diamond. Diamond Relat Mater 96:207–215

Hudson PRW, Tsong IST (1977) Hydrogen impurity in natural gem diamond. J Mater Sci 12:2389–2395

Iakoubovskii K, Kiflawi I, Johnston K, Collins A, Davies G, Stesmans A (2003) Annealing of vacancies and interstitials in diamond. Physica B, 340–342:67–75

Jones R, Goss JP, Briddon PR (2009) Acceptor level of nitrogen in diamond and the 270-nm absorption band. Phys Rev B 80:033205

Jones R, Goss JP, Pinto H, Palmer DW (2015) Diffusion of nitrogen in diamond and the formation of A-centres. Diamond Relat Mater 53:35–39

Khan RUA, Martineau PM, Cann BL, Newton ME, Twitchen DJ (2009) Charge transfer effects, thermo and photochromism in single crystal CVD synthetic diamond. J Phys: Condens Matter 21:364214

Khan RUA, Martineau PM, Cann BL, Newton ME, Dhillon HK, Twitchen DJ (2010) Color alterations in CVD synthetic diamond with heat and UV exposure: implications for color grading and identification. Gems Gemol 46:18–27

Khan RUA, Cann BL, Martineau PM, Samartseva J, Freeth JJP, Sibley SJ, Hartland CB, Newton ME, Dhillon HK, Twitchen DJ (2013) Colour-causing defects and their related optoelectronic transitions in single crystal CVD diamond. J Phys: Condens Matter 25:275801

Khong YL, Collins AT, Allers L (1994) Luminescence decay time studies and time-resolved cathodoluminescence spectroscopy of CVD diamond. Diamond Relat Mater 3:1023–1027

Kiflawi I, Bruley J (2000) The nitrogen aggregation sequence and the formation of voidites in diamond. Diamond Relat Mater 9:87–93

Kiflawi I, Mainwood A (1996) Nitrogen interstitials in diamond. Phys Rev B 54:16719

Kiflawi I, Sittas G, Kanda H, Fisher D (1997) The irradiation and annealing of Si-doped diamond single crystals. Diamond Relat Mater 6:146–148

Kiflawi I, Bruley J, Luyten W, Van Tendeloo G (1998) 'Natural' and 'man-made' platelets in Type-Ia diamonds. Philos Mag B 78:299–314

King JM, Moses TM, Shigley JE, Welbourn CM, Lawson SC, Cooper M (1998) Characterizing natural-color Type IIb blue diamonds. Gems Gemol 34:246–268

King JM, Shigley JE, Gelb TH, Guhin SS, Hall M, Wang W (2005) Characterization and grading of natural-color yellow diamonds. Gems Gemol 41:88–115

King JM, Geurts RH, Gilbertson AM, Shigley JE (2008) Color grading "D-to-Z" diamonds at the GIA Laboratory. Gems Gemol 44:296–321

Klein PB, Crossfield MD, Freitas JA, Collins AT (1995) Donor-acceptor pair recombination in synthetic Type-IIb semiconducting diamond. Phys Rev B 51:9634–9642

Kohn SC, Speich L, Smith CB, Bulanova GP (2016) FTIR thermochronometry of natural diamonds: A closer look. Lithos 265:148–158

Kupriyanov IN, Gusev VA, Borzdov YM, Kalinin AA, Palyanov YN (1999) Photoluminescence study of annealed nickel- and nitrogen-containing synthetic diamond. Diamond Relat Mater 8:1301–1309

Kupriyanov IN, Gusev VA, Pal'yanov YN, Borzdov YM, Sokol AG (2001) Photoluminescence excitation study of cobalt-related optical centers in high-pressure high-temperature diamond. Diamond Relat Mater 10:59–62

Lai MY, Stachel T, Breeding CM, Stern R (2019) Yellow diamonds with colourless cores—evidence for episodic diamond growth beneath Chidliak and the Ekati mine, Canada. Mineral Petrol 114:91–103

Lawson SC, Kanda H (1993) An annealing study of nickel point defects in high-pressure synthetic diamond. J Appl Phys 73:3967–3973

Lawson SC, Kanda H, Watanabe K, Kiflawi I, Sato Y, Collins AT (1996) Spectroscopic study of cobalt-related optical centers in synthetic diamond. J Appl Phys 79:4348–4357

Lawson SC, Fisher D, Hunt DC, Newton ME (1998) On the existence of positively charged single-substitutional nitrogen in diamond. J Phys: Condens Matter 10:6171–6180

Liggins S, Newton ME, Goss JP, Briddon PR, Fisher D (2010) Identification of the dinitrogen <001>-split interstitial H1a in diamond. Phys Rev B 81:085214

Lim H, Park S, Cheong H, Choi HM, Kim YC (2010) Discrimination between natural and HPHT-treated Type IIa diamonds using photoluminescence spectroscopy. Diamond Relat Mater 19:1254–1258

Loubser JHN, van Wyk JA (1978) Electron spin resonance in the study of diamond. Rep Prog Phys 41:1201–1248

Loubser JHN, van Wyk JA (1981) Models for the H3 and H4 centres based on ESR measurements. *In:* 32nd Diamond Conference. Diamond Conference, Reading

Loudin LC (2017) Photoluminescence mapping of optical defects in HPHT synthetic diamond. Gems Gemol 53:180

Lühmann T, Raatz N, John R, Lesik M, Rödiger J, Portail M, Wildanger D, Kleißler F, Nordlund K, Zaitsev A, Roch JF (2018) Screening and engineering of colour centres in diamond. J Phys D: Appl Phys 51:483002

Macpherson JV (2015) A practical guide to using boron doped diamond in electrochemical research. Phys Chem Chem Phys 17:2935–2949

Mäki J-M, Tuomisto F, Kelly CJ, Fisher D, Martineau PM (2009) Properties of optically active vacancy clusters in Type IIa diamond. J Phys: Condens Matter 21:364216

Mäki J-M, Tuomisto F, Varpula A, Fisher D, Khan RUA, Martineau PM (2011) Time dependence of charge transfer processes in diamond studied with positrons. Phys Rev Letters 107:217403

Manson NB, Hedges M, Barson MSJ, Ahlefeldt R, Doherty MW, Abe H, Ohshima T, Sellars MJ (2018) NV–N⁺ pair centre in 1b diamond. New J Phys 20:113037

Mendelssohn MJ, Milledge HJ (1995) Geologically significant information from routine analysis of the mid-infrared spectra of diamonds. Int Geol Rev 37:95–110

Meng YF, Yan CS, Lai J, Krasnicki S, Shu H, Yu T, Liang Q, Mao HK, Hemley RJ (2008) Enhanced optical properties of chemical vapor deposited single crystal diamond by low-pressure/high-temperature annealing. PNAS 105:17620–17625

Nadolinny V, Komarovskikh A, Palyanov Y (2017) Incorporation of large impurity atoms into the diamond crystal lattice: EPR of split-vacancy defects in diamond. Crystals 7:237

Nadolinny VA, Yelisseyev AP (1994) New paramagnetic centres containing nickel ions in diamond. Diamond Relat Mater 3:17–21

Nadolinny VA, Yelisseyev AP, Baker JM, Newton ME, Twitchen DJ, Lawson SC, Yuryeva OP, Feigelson BN (1999) A study of ¹³C hyperfine structure in the EPR of nickel-nitrogen-containing centres in diamond and correlation with their optical properties. J Phys: Condens Matter 11:7357–7376

Nadolinny VA, Yelisseyev AP, Baker JM, Twitchen DJ, Newton ME, Feigelson BN, Yuryeva OP (2000) Mechanisms of nitrogen aggregation in nickel- and cobalt-containing synthetic diamonds. Diamond Relat Mater 9:883–886

Nadolinny VA, Baker JM, Yuryeva OP, Newton ME, Twitchen DJ, Palyanov YN (2005) EPR study of the peculiarities of incorporating transition metal ions into the diamond structure. Appl Magn Reson 28:365–381

Nasdala L, Grambole D, Wildner M, Gigler AM, Hainschwang T, Zaitsev AM, Harris JW, Milledge J, Schulze DJ, Hofmeister W, Balmer WA (2013) Radio-colouration of diamond: A spectroscopic study. Contrib Mineral Petrol 165:843–861

Navon O, Wirth R, Schmidt C, Jablon BM, Schreiber A, Emmanuel S (2017) Solid molecular nitrogen (δ-N2) inclusions in Juina diamonds: Exsolution at the base of the transition zone. Earth Planet Sci Lett 464:237–247

Newton ME (1994) Electron paramagnetic resonance of radiation damage centres in diamond. *In:* Properties and Growth of Diamond. G Davies (Ed.), IEE/INSPEC, p. 153–158

Newton ME, Campbell BA, Twitchen DJ, Baker JM, Anthony TR (2002) Recombination-enhanced diffusion of self-interstitial atoms and vacancy–interstitial recombination in diamond. Diamond Relat Mater 11:618–622

Nimis P (2022) Pressure and temperature data for diamonds. Rev Mineral Geochem 88:533–566

Overton TW, Shigley JE (2008) A history of diamond treatments. Gems Gemol 44:32–55

Peaker CV, Atumi MK, Goss JP, Briddon PR, Horsfall AB, Rayson MJ, Jones R (2016) Assignment of ¹³C hyperfine interactions in the P1-center in diamond. Diamond Relat Mater 70:118–123

Pezzagna S, Rogalla D, Wildanger D, Meijer J, Zaitsev A (2011) Creation and nature of optical centres in diamond for single-photon emission-overview and critical remarks. New J Phys, 13: 035024

Pinto H, Jones R, Palmer DW, Goss JP, Briddon PR, Öberg S (2012) On the diffusion of NV defects in diamond. Phys status solidi (a) 209:1765–1768

Reinitz IM, Buerki PR, Shigley JE, McClure SF, Moses TM (2000) Identification of HPHT-treated yellow to green diamonds. Gems Gemol 36:128–137

Rondin L, Tetienne J-P, Hingant T, Roch J-F, Maletinsky P, Jacques V (2014) Magnetometry with nitrogen-vacancy defects in diamond. Rep Prog Phys 77:056503

Rosch S (1957) Das Grune Gewölbe in Dresden. Z Dtsch Ges Edelsteinkunde, Sonderheft, p. 79–84

Rudloff-Grund J, Brenker FE, Marquardt K, Howell D, Schreiber A, O'Reilly SY, Griffin WL, Kaminsky FV (2016) Nitrogen nanoinclusions in milky diamonds from Juina area, Mato Grosso State, Brazil. Lithos 265:57–67

Smit KV, Shirey SB, Wang W (2016) Type Ib diamond formation and preservation in the West African lithospheric mantle: Re–Os age constraints from sulphide inclusions in Zimmi diamonds. Precambrian Res 286:152–166

Smith W, Sorokin P, Gelles I, Lasher G (1959) Electron-spin resonance of nitrogen donors in diamond. Phys Rev 115:1546–1552

Smith HE, Davies G, Newton ME, Kanda H (2004) Structure of the self-interstitial in diamond. Phys Rev B 69:045203

Smith EM, Shirey SB, Nestola F, Bullock ES, Wang J, Richardson SH, Wang W (2016) Large gem diamonds from metallic liquid in Earth's deep mantle. Science 354:1403–1405

Smith EM, Shirey SB, Richardson SH, Nestola F, Bullock ES, Wang J, Wang W (2018) Blue boron-bearing diamonds from Earth's lower mantle. Nature 560:84–87

Solin SA, Ramdas AK (1970) Raman spectrum of diamond. Phys Rev B 1:1687–1698

Speich L, Kohn SC, Bulanova GP, Smith CB (2018) The behaviour of platelets in natural diamonds and the development of a new mantle thermometer. Contrib Mineral Petrol 173:39

Stacey A, Karle TJ, McGuinness LP, Gibson BC, Ganesan K, Tomljenovic-Hanic S, Greentree AD, Hoffman A, Beausoleil RG, Prawer S (2012) Depletion of nitrogen-vacancy color centers in diamond via hydrogen passivation. Appl Phys Lett 100:071902

Stachel T, Harris JW (2008) The origin of cratonic diamonds—Constraints from mineral inclusions. Ore Geol Rev 34:5–32

Stachel T, Luth RW (2015) Diamond formation —Where, when and how? Lithos, 220–223:200–220

Steele JA, Puech P, Lewis RA (2016) Polarized Raman backscattering selection rules for (hhl)-oriented diamond- and zincblende-type crystals. J Appl Phys 120:055701

Sumida N, Lang AR (1981) Cathodoluminescence evidence of dislocation interactions in diamond. Philos Mag A 43:1277–1287

Tallaire A, Collins AT, Charles D, Achard J, Sussmann R, Gicquel A, Newton ME, Edmonds AM, Cruddace RJ (2006) Characterisation of high-quality thick single-crystal diamond grown by CVD with a low nitrogen addition. Diamond Relat Mater 15:1700–1707

Tallaire A, Achard J, Silva F, Brinza O, Gicquel A (2013) Growth of large size diamond single crystals by plasma assisted chemical vapour deposition: Recent achievements and remaining challenges. C R Phys 14:169–184

Tallaire A, Lesik M, Jacques V, Pezzagna S, Mille V, Brinza O, Meijer J, Abel B, Roch JF, Gicquel A, Achard J (2015) Temperature dependent creation of nitrogen-vacancy centers in single crystal CVD diamond layers. Diamond Relat Mater 51:55–60

Tang CJ, Neves AJ, Carmo MC (2005) On the two-phonon absorption of CVD diamond films. Diamond Relat Mater 14:1943–1949

Taylor WR, Jaques AL, Ridd M (1990) Nitrogen-defect aggregation characteristics of some Australasian diamonds: time-temperature constraints on the source regions of pipe and alluvial diamonds. Am Mineral 75:1290–1310

Taylor WR, Canil D, Milledge HJ (1996) Kinetics of Ib to IaA nitrogen aggregation in diamond. Geochimica et Cosmochimica Acta 60:4725–4733

Themelis T (1987) Diamonds from Venezuela. Lapidary Journal 41:59–64

Twitchen D, Newton M, Baker J, Tucker O, Anthony T, Banholzer W (1996) Electron-paramagnetic-resonance measurements on the di-<001>-split interstitial center (R1) in diamond. Phys Rev B 54:6988–6998

Twitchen DJ, Hunt DC, Smart V, Newton ME, Baker JM (1999) Correlation between ND1 optical absorption, the concentration of negative vacancies determined by electron paramagnetic resonance (EPR). Diamond Relat Mater 8:1572–1575

van der Bogert C, Smith C, Hainschwang T, Mcclure S (2009) Gray-to-blue-to-violet hydrogen-rich diamonds from the Argyle Mine, Australia. Gems Gemol 45:20–37

van Wyk JA, Loubser JHN (1993) ENDOR of the P2 centre in type-Ia diamonds. J Phys: Condens Matter 5:3019–3026

van Wyk JA, Woods GS (1995) Electron spin resonance of excited states of the H3 and H4 centres in irradiated type Ia diamonds. J Phys: Condens Matter 7:5901–5911

Vance ER, Milledge HJ (1972) Natural and laboratory α -particle irradiation of diamond. Minerall Mag 38:878–881

Vance ER, Harris JW, Milledge HJ (1973) Possible origins of α-damage in diamonds from kimberlite and alluvial sources. Mineral Mag 39:349–360

Walker J (1977) An optical study of the TR12 and 3H defects in irradiated diamond. J Phys C: Solid State Phys 10:3031–3037

Walker J (1979) Optical absorption and luminescence in diamond. Rep Prog Phys 42:1605–1659

Walsh PS, Lightowlers EC, Collins AT (1971) Thermoluminescence and phosphorescence in natural and synthetic semiconducting diamond. J Lumin 4:369–392

Walter B (1891) Eine charakteristiche Absorptionserscheinung des Diamanten. Ann Physik Chem 3:42, 504–510.[1]

Wang W, D'Haenens-Johansson UFS, Johnson P, Moe KS, Emerson E, Newton ME, Moses TM (2012) CVD synthetic diamonds from Gemesis Corp. Gems Gemol 48:80–97

Wassell AM, McGuinness CD, Hodges C, Lanigan PMP, Fisher D, Martineau PM, Newton ME, Lynch SA (2018) Anomalous green luminescent properties in CVD synthetic diamonds. Phys Status Solidi A 215:1800292

Watanabe K, Lawson SC, Isoya J, Kanda H, Sato Y (1997) Phosphorescence in high-pressure synthetic diamond. Diamond Relat Mater 6:99–106

Wedepohl PT (1957) Electrical and optical properties of Type IIb diamonds. Proc Phys Soc Sect B 70:177–185

Wight DR, Dean PJ, Lightowlers EC, Mobsby CD (1971) Luminescence from natural and man-made diamond in the near infrared. J Lumin 4:169–193

Woods GS (1984) Infrared absorption studies of the annealing of irradiated diamonds. Philos Mag B 50:673–688

Woods GS (1986) Platelets and the infrared Absorption of Type Ia Diamonds. Proc R Soc London, Ser A 407:219–238

Woods GS, Purser GC, Mtimkulu ASS, Collins AT (1990a) The nitrogen content of Type Ia natural diamonds. J Phys Chem Solids 51:1191–1197

Woods GS, Van Wyk JA, Collins AT (1990b) The nitrogen content of Type Ib synthetic diamond. Philos Mag Part B 62:589–595

Yelisseyev AP, Kanda H (2007) Optical centers related to 3d transition metals in diamond. New Diamond Front Carbon Technol 17:127

Zaitsev AM (2001) Optical Properties of Diamond. Springer

Zaitsev AM, Moe KS, Wang W (2018) Defect transformations in nitrogen-doped CVD diamond during irradiation and annealing. Diamond Relat Mater 88:237–255

---

[1] Series 3, volume 42, edited by G. Wiedemann, and also known as Wiedemann's Annalen, is volume 278 (issue 3) in the Wiley online archive.